NAVAL POSTGRADUATE SCHOOL
Monterey , California

THESIS

H47265

MONTE CARLO CALCULATION OF ELECTRON
MULTIPLE SCATTERING IN THIN FOILS

by

Daniel Christian Jensen

June 1988

Thesis Advisor   X.K. Maruyama

REPORT DOCUMENTATION PAGE

1a Report Security Classification Unclassified			1b Restrictive Markings			
2a Security Classification Authority			3 Distribution Availability of Report			
2b Declassification Downgrading Schedule			Approved for public release; distribution is unlimited.			
4 Performing Organization Report Number(s)			5 Monitoring Organization Report Number(s)			
6a Name of Performing Organization Naval Postgraduate School		6b Office Symbol (if applicable) 33	7a Name of Monitoring Organization Naval Postgraduate School			
6c Address (city, state, and ZIP code) Monterey, CA 93943-5000			7b Address (city, state, and ZIP code) Monterey, CA 93943-5000			
8a Name of Funding Sponsoring Organization		8b Office Symbol (if applicable)	9 Procurement Instrument Identification Number			
8c Address (city, state, and ZIP code)			10 Source of Funding Numbers			
			Program Element No	Project No	Task No	Work Unit Accession No

11 Title (include security classification) MONTE CARLO CALCULATION OF ELECTRON MULTIPLE SCATTERING IN THIN FOILS

12 Personal Author(s) Daniel Christian Jensen

13a Type of Report Master's Thesis	13b Time Covered From To	14 Date of Report (year, month, day) June 1988	15 Page Count 90

16 Supplementary Notation The views expressed in this thesis are those of the author and do not reflect the official policy or position of the Department of Defense or the U.S. Government.

17 Cosati Codes			18 Subject Terms (continue on reverse if necessary and identify by block number)
Field	Group	Subgroup	Multiple Scattering, ITS CYLTRAN, Monte Carlo

19 Abstract (continue on reverse if necessary and identify by block number)

The electron photon transport code ITS has many applications in the physics and medical industries. The code was originally intented for use in determining particle transport in thick materials. The code breaks down for very thin targets because the multiple scattering approximation used to determine the electron deflection angles for thin steps is inadequate. A method of correction has been developed by Tom Jordan and Joseph Mack which combines a small angle approximation theory to the multiple scattering and an explicit large angle treatment based on a Poisson distribution. This method has been validated against several experiments with great success. The multiple scattering theory of Moliere has also been incorporated into a correction scheme and shows good agreement with experimental data.

20 Distribution Availability of Abstract ☒ unclassified unlimited ☐ same as report ☐ DTIC users	21 Abstract Security Classification Unclassified	
22a Name of Responsible Individual X.K. Maruyama	22b Telephone (include Area code) (408) 646-2431	22c Office Symbol 54Ss

DD FORM 1473,84 MAR   83 APR edition may be used until exhausted   security classification of this page
All other editions are obsolete

Monte Carlo Calculation of Electron Multiple Scattering in Thin Foils

by

Daniel Christian Jensen
Lieutenant, United States Navy Reserve
B.S., Michigan State University, 1983

Submitted in partial fulfillment of the
requirements for the degree of

MASTER OF SCIENCE IN PHYSICS

from the

NAVAL POSTGRADUATE SCHOOL
June 1988

ABSTRACT

The electron photon transport code ITS has many applications in the physics and medical industries. The code was originally intented for use in determining particle transport in thick materials. The code breaks down for very thin targets because the multiple scattering approximation used to determine the electron deflection angles for thin steps is inadequate. A method of correction has been developed by Tom Jordan and Joseph Mack which combines a small angle approximation theory to the multiple scattering and an explicit large angle treatment based on a Poisson distribution. This method has been validated against several experiments with great success. The multiple scattering theory of Moliere has also been incorporated into a correction scheme and shows good agreement with experimental data.

TABLE OF CONTENTS

LIST OF TABLES

LIST OF FIGURES

vii

ACKNOWLEDGEMENTS

I. INTRODUCTION

Particle transport dates back to the days of Lord Rutherford when the scattering of electrons through thin foils changed our view of the nature of matter. Today particle transport through matter is itself an industry. From determining the radiation damage effects on satellites in space to calculating the energy spectrum of medical x-ray machines, particle scattering is an important part of the science industry. In the past only rigorous experimention provided scattering information for the scientist. Today with the aid of high speed computers and a better understanding of the various particle interactions, computational results can be easily obtained. Computer programs which model the transport of particles through matter were developed around 1968. M. Berger and S. Seltzer at the National Bureau of Standards developed the first general electron and photon transport code called ETRAN. From 1970 to 1981 eleven codes based on the ETRAN model were developed, and in 1984 eight of these codes were combined into single code package called the Integrated Tiger Series (ITS). The eight codes differ in dimensional geometry and two of the codes include transport in macroscopic electric and magnetic fields [Ref. 1: p. 6].

Electron and photon transport computer codes such as ETRAN were originally developed to study the manner in which radiation scatters through thick materials. Quantities such as energy deposition and angular deflection are calculated using various Monte Carlo schemes. Such schemes are based on condensed case histories, that is, a particle's energy, direction, and position are calculated at discrete intervals rather than continuously as the particle traverses the medium. Probability distribution functions based on this interval are then used to determine the state of the particle after each step. This scheme has been very successful in the study of thick target particle transport. Recently, these transport codes have been applied to very thin foils for transition radiation research. Discrepancies in the angular distribution of the transmitted electrons resulted which indicate an apparent break-down in the code calculation of the multiple scattering.

The multiple scattering distribution is based on a substep size which is calculated from the particles radiation length and the target material density. Berger [Ref. 2: p. 143] has pointed out three advantages for small step sizes, two of which affect the angular distribution of the particles. If the step size is small, the majority of the scattering is

done within the material and boundary effects need only be calculated in the partial substep at the escaping edge. The scattering in the partial substep will have a small impact on the total angular deflection so that crude approximations to the multiple scattering can be used for this region. The net angular deflection within a substep is so minimal that multiple scattering theories with this restriction are applicable. For thick materials where the number of collisions is large, these assumptions are valid. The majority of the scattering is done within the boundary of the material and the overall distribution is calculated in this region. The number of collisions in the final substep is so small that their contribution to the overall angular distribution is minimal. However, for very thin materials, where the thickness is less than the substep size, the entire scattering distribution is determined from the crude approximation.

The number of collisions presents another problem in the calculation of the angle deflection. Small angle approximate multiple scattering theories ignore the large angle calculation because if the number of collisions is large the majority of the scattering will be small angle scattering. For very thin materials the number of collisions can be so small that an occasional large angle scatter can make a large contribution to the overall angle distribution. It is therefore necessary to develop the large angle scattering distribution along with the small angle profile.

The Integrated Tiger Series of coupled photon and electron transport codes (ITS) were originally developed for thick material transport. When the ITS code for cylindrical geometry (CYLTRAN) was used for very thin free standing foils, the angular distribution of the transmitted electrons had broader Gaussian forms then that of the available experimental data. The need for a correction to the multiple scattering distribution for very thin materials existed, and several methods of solution were considered.

The best method of correction would be an explicit treatment of the scattering based on the screened Rutherford cross section whereby each electron collision deflection angle is calculated as the particle is stepped through the material. Although this method would give very accurate results the time inefficiency makes it impractical for computer programing. Any other treatment would require a theory of multiple scattering to determine the angular distribution. The five principle works on the subject are by Williams [Ref. 3], Goudsmit-Saunderson [Ref. 4], Moliere [Ref. 5], Synder-Scott [Ref. 6], and Lewis [Ref. 7]. The theories at a glance seem as diverse as the random processes

2

themselves; however, in the limit of small angles they are essentially the same. A brief history of the evolution of these theories will serve to amplify this point.

When charged particles are incident on a slab, the distribution of the scattered particles is described by the well-known Boltzman integro-differential equation. Bothe [Ref. 8: p. 11] showed that in the limit of small angles, this equation transforms into a Fokker-Planck type differential equation. Although his own theory of multiple scattering was flawed with inexact boundary conditions and approximations, the Bothe-Fokker-Planck general form for the distribution would become the standard form for all small angle approximation theories which would follow.

Williams was the first to utilize the Fokker-Planck equation successfully. Although his expression for the angular deflection showed agreement with the experimental data of the time, his theory would be overshadowed by the historic Goudsmit-Saunderson theory which was published one year later. The Goudsmit-Saunderson theory was an exact treatment based on a Legendre polynominal expansion and was valid for all angles. The theory was exact except for the assumption of equal path lengths.

Almost a decade followed before another theory of multiple scattering was published, and that was the theory of Moliere. Moliere used small angle approximations to transform the standard transport equation into a form which resembled diffusion. He then expanded the resulting expression in terms of an iteration constant to evaluate the distribution. The Moliere theory showed great agreement with experimental data, especially for thin materials, and is the standard theoretical comparison for all scattering experiments today. Another small angle approximation shortly followed by Synder-Scott which effectively derived the Moliere integral equation from a standard diffusion equation. A year later Lewis showed that the integro-differential equation for small angles conformed to the Synder-Scott expression. Finally Nigam, Saunderson, and Ya-You Wu [Ref. 9: p. 1092] showed the equivalence of the Moliere and the Goudsmit-Saunderson theory in the limit of small angles.

In the present paper, we are concerned with scattering in very thin materials, where the scattering angles are small. Therefore the small angle approximation theories of Williams and Moliere are appropriate. Even with the best possible multiple scattering theory, the question of large angle deflections still remains. With very thin materials the number of collisions is so small that the occasional large angle scatter makes a significant contribution and cannot be ignored.

A method of solution has been developed by Thomas Jordan and Joseph Mack which combines the small angle theory of Williams and an explicit treatment of the large angle scattering. Chapter two will outline the theories of Williams, Goudsmit-Saunderson, and Moliere. Chapters three and four will describe the multiple scattering algorithm in the existing ITS code CYLTRAN and the correction scheme by Jordan-Mack.

II. THEORY

A. WILLIAMS

The particle scattering theory by E.J. Williams was the first theory to properly use the Fokker-Planck equation. As pointed out by Bothe [Ref. 8: p. 164] a particular solution to the Fokker-Planck equation for multiple scattering has a Gaussian form. Williams states the same relation with reference to the general theory of errors. The difference between Bothe and Williams is that Williams limited the scattering angle to a finite value. In addition Williams set the cosine of the scattering angle equal to unity, whereas Bothe kept the cosine term in his solution of the scattering cross section.

To determine the multiple scattering distribution function Williams defined a limiting angle ϕ_1 such that on the average the particle would deflect once through an angle greater than ϕ_1 while traversing the material. This can be written by setting the number of collisions in the back region equal to unity:

$$\int_{\phi_1}^{\pi} P(\phi)\, d\phi = 1 \tag{3.1}$$

where $P(\phi)$ is the collision cross section. Since virtually all the scattering is done at an angle less then ϕ_1 an approximation to the total distribution can be found by considering the deflections in this region. Williams showed that from the general theory of errors, the probability of scattering into an angle α_1, of a particle due to collisions which are less than ϕ_1 can be represented by a Gaussian of the form:

$$P_1(\alpha_1)\, d\alpha_1 = \left(\frac{2}{\pi\bar{\alpha}_1} \right) \exp\left[\frac{-\alpha_1^2}{\pi\bar{\alpha}_1^2} \right] d\alpha_1 \tag{3.2}$$

where $\bar{\alpha}_1^2$ is the arithemetic mean value of α_1 and is given by:

$$\bar{\alpha}_1^2 = \frac{2}{\pi} \int_0^{\phi_1} \phi^2 P(\phi)\, d\phi \tag{3.3}$$

5

This general form of the theory is a good approximation to the multiple scattering; however, when Williams derived it he used the unscreened Rutherford cross section with the small angle approximations $2 \sin \frac{1}{2}\theta \sim \theta$, and $\cos \frac{1}{2}\theta \sim 1$ which resulted in:

$$P(\phi) = \frac{4\pi N t Z^2 e^4}{M^2 c^4 \beta^4 \xi^2 \phi^3} \tag{3.4}$$

where N is the number of scattering atoms, t is the thickness of the scatterer, Z is the charge of the particle, M is the mass of the particle, $\beta = (v/c)$, and $\xi = (\sqrt{1 - \beta^2})^{-1}$. In addition, he further modified $\bar{\alpha}_1^2$ by an approximation to take into account the screening of the atomic electrons. To graph his distribution Williams defined a unit of angle which would become the "natural" angle for several papers on multiple scattering. The angle is given by:

$$\delta^2 = \frac{N t Z e^2}{M c^2 \beta^2 \xi} \tag{3.5}$$

Originally, Williams was concerned with thick targets, fast particles, and unit charges. In his second paper he modified $\bar{\alpha}_1^2$ to avoid second-order approximations he used in the original derivation. This modification extended his theory to thinner targets (0.01 cm).

B. GOUDSMIT-SAUNDERSON

The multiple scattering theory of Goudsmit-Saunderson is often quoted as an "exact" theory and in the development of the most general form of the theory no assumptions or approximations are used. However, in the derivation of the collision cross section an assumption of small angles and equal path lengths is asserted such that the resulting distribution is a small angle approximation. The theory is founded in the basic Legendre polynomial property that the average value of any polynomial after n events is equal to the average value of the polynomials after one event to the nth power:

$$< P_n(\cos \theta) >_{av} = < P_1(\cos \theta_\xi) >_{av}^n \tag{3.6}$$

where θ is the final scattered angle after several collisions, and θ_ξ is the scattered angle after one collision. The total average of any Legendre polynomial can be written as:

$$G_l = \sum_{n=0}^{\infty} W(n) < P_1(\cos \theta_\xi) >_{av}^n \tag{3.7}$$

The scattering distribution is then given by summing all these averages per unit solid angle:

$$f(\theta) = \frac{1}{4\pi} \sum (2l + 1) G_l P_l(\cos \theta) \tag{3.8}$$

The collision probability can be represented by a Poisson distribution which has functional dependence on the total collision cross section ρ , and the thickness of the scatterer t:

$$W(n) = \frac{e^{-v} v^n}{n!} \; ; v = \pi \rho^2 N t \tag{3.9}$$

This expression would be exact if the true path length were equal to the foil thickness, and for small deflections this assumption is quite valid.

The evaluation of the Goudsmit-Saunderson theory has been developed extensively by Spenser [Ref. 10] and Berger [Ref. 2: p. 207]. The Goudsmit-Saunderson multiple scattering distribution is given by Berger as

$$A_{GS}(\omega) = \sum_{l=0}^{\infty} (l + \tfrac{1}{2}) \exp\left[-\int_0^s G_l(s') \, ds' \right] P_l(\cos \omega) \tag{3.10}$$

The expansion coefficients G_l are given by:

$$G_l = 2\pi N \int_0^\pi \sigma(\theta)\{1 - P_l(\cos \theta)\} \sin \theta \, d\theta \tag{3.11}$$

where $\sigma(\theta)$ is the screened Rutherford cross section which has the form:

$$\sigma(\theta) = \frac{Z^2 e^4}{p^2 v^2 (1 - \cos \theta + 2\eta)^2} \tag{3.12}$$

$$\eta = \tfrac{1}{4} \chi_a^2 \tag{3.13}$$

The constant χ_a^2 is Moliere's screening angle and is given by equation (3.21). To solve equation (3.10), recursion relations are developed so that a large number of expansion coefficients can be calculated. Berger [Ref. 2: p. 213] shows that a convenient form of

7

the distribution for random sampling can be found by replacing the Legendre polynomials $P_l(\cos \omega)$ by the relation:

$$H_l(\cos \omega) = \int_{\cos \omega}^{1} P_l(x)\, dx \tag{3.14}$$

with the recursion relations:

$$H_0 = 1 - \cos \omega \tag{3.15}$$

$$H_1 = \tfrac{1}{2}(1 - \cos^2 \omega) \tag{3.16}$$

$$(l + 1)H_l = (2l - 1)\cos \omega H_{l-1} - (l - 2)H_{l-2} \quad l \geq 2 \tag{3.17}$$

This method of solution to the Goudsmit-Saunderson theory is used in the ITS code system for the multiple scattering within the material.

C. MOLIERE

Moliere takes a different approach in that he explicitly starts his theory with the assumption that all scattering angles are small, such that the standard transport equation reduces to an expression which resembles diffusion in a plane:

$$\frac{\partial f(\theta, t)}{\partial t} = -Nf(\theta, t)\int \sigma(\chi)\chi\, d\chi + N\int f(\theta_p, t)\sigma(\chi)\, dN \tag{3.18}$$

where $\sigma(\chi)$ is the differential scattering cross section, N is the number of scattering atoms per cm^3, $\theta_p = \theta - \chi$, is a vector representing the direction of the electron before the last scatter, $dN = \chi\, d\chi\, d\phi/2\pi$, and $f(\theta, t)$ is the scattering angular distribution. A Fourier (Bessel) transformation which is given in great detail in Bethe's paper produces the angular distribution function of the form:

$$f(\theta, t) = \int_0^\infty \eta\, d\eta J_o(\eta \theta) \times \exp\left[-Nt\int_0^\infty \sigma(\chi)\chi\, d\chi\{1 - J_o(\eta\chi)\}\right] \tag{3.19}$$

where $J_o(\eta\theta)$ and $J_o(\eta\chi)$ are bessel functions of the zeroth order. Moliere takes the theory a step further by transforming his equation into an expression which depends on two angles χ_a^2 and χ_c^2.

The transformed Moliere multiple scattering distribution function then takes the following form:

$$f(\theta)\theta \, d\theta = \lambda \, d\lambda \int_0^\infty y \, dy \, J_o(\lambda_y) \exp\left[\tfrac{1}{4}y^2(-b + \ln \tfrac{1}{4}y^2)\right] \tag{3.20a}$$

$$\lambda = \frac{\theta}{\chi_c} \tag{3.20b}$$

$$b = \ln\left(\frac{6\chi_c}{7\chi_a}\right)^2 \tag{3.20c}$$

$$y = \chi_c \eta \tag{3.20d}$$

The first angle is the screening angle. χ_a^2, which describes the scattering atom and is derived from the specific form of the given scattering law:

$$\chi_a^2 = \left[\frac{(m_ec^2)^2}{(pc)^2}\right]\left[\frac{Z^{\frac{1}{3}}}{(.855 \times 137)}\right]^2\left[1.13 + 3.76\left[\frac{Z}{137\beta}\right]^2\right] \tag{3.21}$$

In Moliere's original paper, he used the Thomas-Fermi potential for the single scattering law. Since this form does not contain the Born approximation only elastic collisions against the Coulomb field of the nucleus was considered. Fano [Ref. 11: p. 117] showed that the correction due to the inelastic collision with atomic electrons consisted of replacing Z^2 by $Z(Z+1)$ and adding an additional term to Moliere's constant b:

$$b = \ln\left(\frac{6\chi_c}{7\chi_a}\right)^2 + (Z+1)^{-1}\{\ln[0.160Z^{-\frac{2}{3}}(1 + 3.33Ze^2/hv)] - c_f\} \tag{3.22}$$

where c_f is an integral over an incoherent scattering function whose value is about -5.0. Berger [Ref. 2: p. 207], extrapolates this constant for several materials which are shown in Figure 1 on page 10.

The second angle is a unit probability angle. χ_c^2, which is a measure of the foil thickness and states that the total probability of a single scatter at an angle greater than χ_c is equal to one.
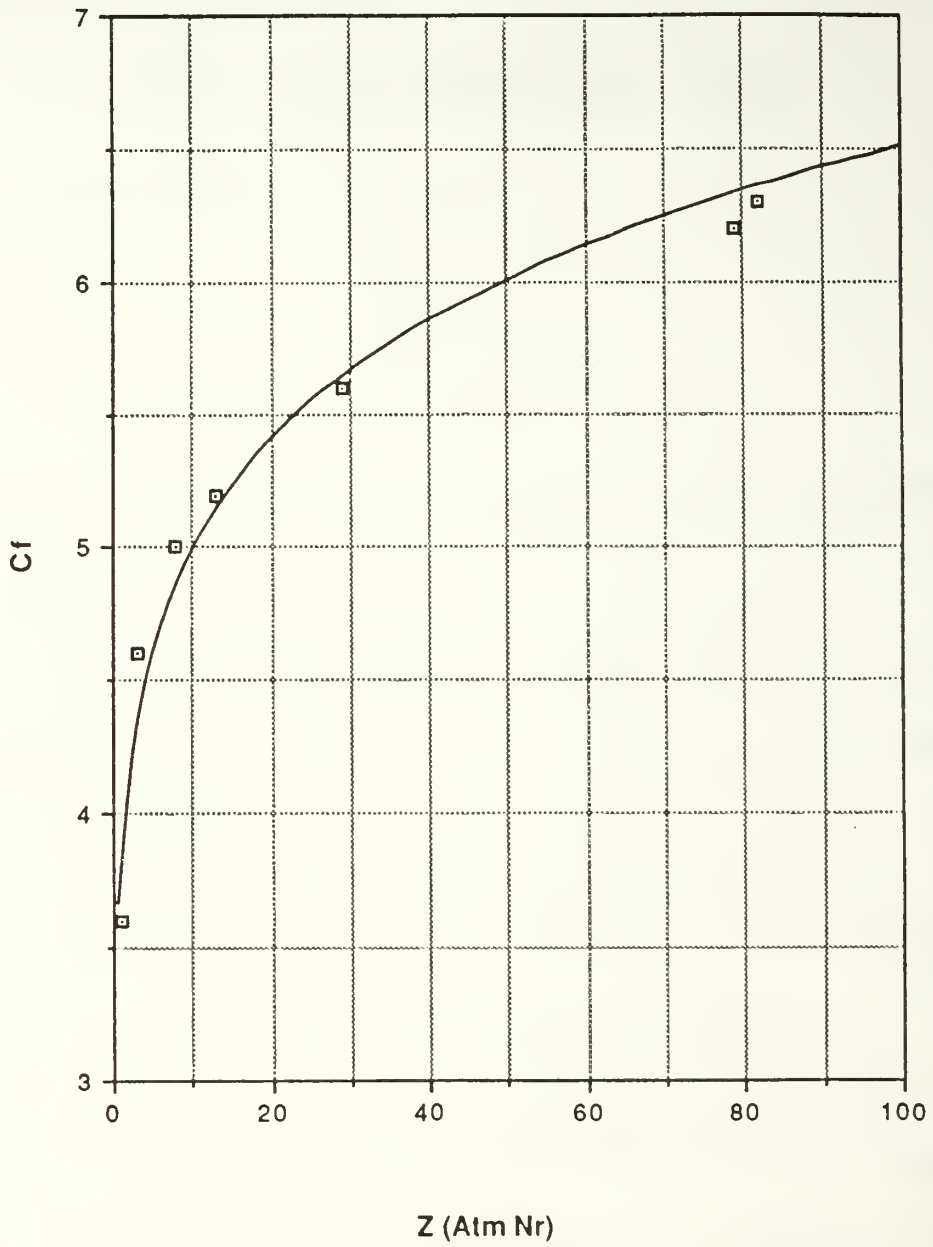
9

Figure 1.   Cf vs Z (Atomic Number):   Fano's correction constant, c, verses atomic number.   Values have been extrapolated from Berger's book, [Ref. 2: p. 207].

This "natural" unit of angle was first determined by Williams in his theory of multiple scattering. The unit probability angle is given as:

$$\chi_c^2 = \frac{4\pi N t e^4 Z(Z+1) z^2}{(pv)^2}$$

(3.23)

To solve the transformed equation Moliere then defines an iteration constant B_m and expands the integral in terms of a power series in $1/B_m$:

$$B_m = b + \ln B_m$$

(3.24)

$$f(\theta)\theta \, d\theta = \xi \, d\xi [f^o(\xi) + B_m^{-1} f^1(\xi) + B_m^{-2} f^2(\xi) + \ldots]$$

(3.25)

where

$$\xi = \frac{\theta}{\xi_c B_m^{1/2}}$$

(3.26)

Moliere's theory is valid for small angles less than thirty degrees [Ref. 12: p. 1256]. His theory can be extended to larger angles by the introduction of a multiplication factor, $\sqrt{\sin \theta / \theta}$, into the overall angular function as suggested by Bethe [Ref. 12: p. 1263]. The first order approximation to the Moliere angular distribution with the correction just mentioned has the following form:

$$f^o \propto \sqrt{\frac{\sin \theta}{\theta}} \, e^{-\frac{\theta^2}{\chi^2 B_m}}$$

(3.27)

This represents the Gaussian term for multiple scattering. Higher order terms are somewhat more difficult to calculate and impractical to program. Bethe indicates that when the scattering is less than two degrees, the second term f^1 , represents a ten percent correction to the Gaussian first term. [Ref. 12: p. 1260]

Since we are concerned with only very thin distances where the scattering is mostly in the forward direction the first term will represent a good approximation to the multiple scattering.

III. ITS (CYLTRAN)

The ITS code CYLTRAN is the transport code for cylindrical geometry. A complete description of the code system is provided in Appendix B. CYLTRAN uses two methods for determining the multiple scattering distribution of the electrons. When the scattering is done within the material, and within a full substep interval, a subroutine named "MULT" is called to calculate the scattered angle of the electron. Subroutine MULT uses the Goudsmit-Saunderson theory to determine the scattering distribution. For scattering in the final partial substep at the escaping edge of the material, a subroutine named "ANGLE" is called. ANGLE uses a crude approximation to the multiple scattering which is described in detail in Appendix C. Both methods hinge around the substep size which depends on the scattering material. The substep size is calculated by the equation:

$$D_{substep} = \frac{D_{RANGE}}{\rho(ISUB)} \tag{4.1}$$

where D_{RANGE} is the mean free path of the incident electron (g cm^2), ISUB is the number of substeps per interval, and ρ is the material density. The scattered angle of the incident electron is then calculated after each substep from the Goudsmit-Saunderson distribution. In a cross section generating program XGEN, the average cosines based on the same substep size given in the equation above, are calculated and stored in an output file. CLYTRAN reads in these stored cosine averages. In a subroutine named MULT the angle distribution is formed using up to 240 Legendre polynominals with the cosine averages. Scattered angles are then drawn from the distribution for each incident electron after each substep. This process works fine until the final substep at the material boundary where the distance from the last full substep to the escaping edge is less than the substep size. In this region the cosine averages calculated by XGEN are no longer valid and the Goudsmit-Saunderson distribution can not be used. To determine the scattering angle distribution a crude approximation to the multiple scattering is used. The approximation is made in a subroutine called ANGLE. ANGLE is called whenever the distance from the last full substep to the escaping edge is less than the substep size.

12

The crude approximation is based on Williams' Gaussian expression:

$$f(\theta) \propto \exp\left(\frac{\theta^2}{\theta_m^2}\right) \sim \exp\left[\frac{(1 - \cos\theta)}{\alpha}\right] \qquad (4.2)$$

where α is calculated from the relation:

$$\alpha = (1 - <\cos\theta>)\frac{SHD}{D_{substep}} \qquad (4.3)$$

The average cosines are given by the program XGEN, and SHD is the distance from the last full substep to the escaping edge. For thick foils this approximation is reasonable because it has very little effect on the total distribution which is calculated from several Goudsmit-Saunderson calculations within the material. For very thin foils where the thickness is less then the step size, the entire angular distribution is determined by this crude approximation. It is therefore necessary to develop a better approximation to the multiple scattering in the final partial substep.

13

IV.   THE JORDAN-MACK CORRECTION

A correction to the multiple scattering distribution which uses the Williams small angle approximation theory and an explicit treatment of large angle scattering has been developed by Thomas Jordan and Joseph Mack.   The major difference between the Jordan and Williams solution is that Jordan uses the Goudsmit-Saunderson expression for the screened Rutherford cross section whereas Williams used the original Rutherford cross section.   The Goudsmit-Saunderson expression is given by:

$$d\sigma = \frac{2\pi e^4 Z^2}{p^2 v^2} \frac{\sin \theta \, d\theta}{(1 - \cos \theta + \tfrac{1}{2}\theta_1^2)^2} \tag{5.1}$$

where θ_1^2 is Moliere's screening angle χ_a^2.   The mean square angle for single scattering is then defined by integrating the average angle over the cross section in the forward region:

$$\omega^2 = Nt \int_0^{\theta_m} \theta^2 \, d\sigma \tag{5.2}$$

where θ_m is defined as the maximum angle such that the probability of a scatter greater than θ_m is exactly one.   Zerby and Keller [Ref. 13: p. 202] state the same relation in their discussion of Moliere's theory, where they assert that the scattering angle must be restricted to exclude large angles for which Moliere's theory breaks down.   To accomplish this, they suggest choosing an angle θ_m such that on the average one large scatter will occur in an angle larger than θ_m.   This method was first derived by Williams almost 27 years earlier.   The small angle approximation is then assumed in the form:

$$\theta^2 = 2(1 - \cos \theta) \tag{5.3}$$

and the resulting mean square angle is given by:

$$\omega^2 = 2Nt \int_0^{\theta_m} (1 - \cos \theta) \, d\sigma \tag{5.4}$$

Equation (5.4) can easily be integrated into the following form:

$$\omega^2 = \chi_c^2 [\chi_d^2 - \ln \chi_d^2 - 1] \qquad (5.5)$$

where $\chi_d^2 = \eta/(1 - \mu_m + \eta)$, $\mu_m = \cos \theta_m$, and $\eta = \frac{1}{2}\theta_1^2 = \frac{1}{2}\chi_a^2$. See Appendix B for the complete proof. The term $(1 - \mu + \eta)$ can be found from the condition that one scatter will occur in the back region:

$$\int_{\theta_m}^{\pi} d\sigma = 1 \qquad (5.6)$$

and upon integration it yields:

$$(1 - \mu_m - \eta) = \frac{1}{\left[\dfrac{2}{\chi_c^2} + \dfrac{1}{2 + \eta} \right]} \qquad (5.7)$$

With the mean square angle completely determined, the Gaussian form of the distribution is known:

$$f \propto e^{\frac{-\theta^2}{\omega^2}} \qquad (5.8)$$

To extend this relation to larger angles the multiplication factor $\sqrt{\overline{\sin \theta / \theta}}$ as suggested by Bethe [Ref. 12: p. 1263] for Moliere's theory can also be incorporated into the previous equation so that the final distribution function has the form:

$$F(\theta) \propto \sqrt{\frac{\sin \theta}{\theta}} \; e^{\frac{-\theta^2}{\omega^2}} \qquad (5.9)$$

For a given electron scatter through a material distance t, the small angle deflection can be determined from the distribution function $F(\theta)$: however, the large angle deflection must also be determined. To accomplish this, a Poisson distribution function is constructed whereby each term represents the probability of a large angle scatter:

$$P_n = \frac{m^n}{n!} e^{-m} \qquad (5.10)$$

where m is the probability of a single event. Since the expected number of collisions in the back region, $(\theta > \theta_m)$ has been set to unity, the probability of a single event is equal to one, (i.e. m = 1). A random number can then be drawn and the probability of each

15

individual large angle scatter subtracted from it until the remaining probability is less than or equal to zero. For each large angle scatter an explicit random angle determination is done based on the collision cross section. The Poisson distribution can only be used when the scattering probability is small and constant as in the case of very thin foils. If the foil is too thick or the energy of the incident electron is too small, then the probability of large angle scattering will increase and Poisson statistics will not properly described the distribution.

Thus the multiple scattering has been decoupled into small and large angle scattering. This technique hinges around the angle parameter θ_m, the maximum angle for which one large scatter will occur at an angle greater than θ_m. In the case of ultra thin foils or very high energy electrons it may not be possible to have a large angle scatter. In this case $\cos \theta_m$ turns out to be greater than one! Therefore it is necessary to calculate the angle deflection by the explicit Poisson treatment for all collisions within a step size. For this case the probability of a single event m is equal to the total collision cross section integrated over all angles:

$$m = Nt \int_0^\pi d\sigma \qquad (5.11)$$

V. RESULTS

The Moliere and Jordan-Mack correction schemes were programed into the ITS code CYLTRAN by inserting a call statement in subroutine ANGLE. This statement calls a new subroutine ANGDET (ANGle DETermine) which contains the correction schemes. When the distance from the last full substep to the escaping edge is less than the substep size, ANGLE is called by the main program and ANGDET is called by ANGLE. The fortran source code for both corrections is given in Appendix C, along with the existing ANGLE subroutine code. The input parameters to CYLTRAN for each run where similar to the example input file given in Appendix B. The number of histories for each run was 100,000. The statistics for each run were calculated based on ten batches.

The problem of validating and comparing the existing CYLTRAN code with the two correction schemes was difficult due to the lack of sufficient experimental data for scattering through very thin foils. Originally only the historic results of Hanson [Ref. 14: p. 634] were considered. In this experiment Hanson used a 18.66 mg cm² (9.67 × ;f.10⁻⁴cm) gold foil with 15.77 MeV electrons. Figure 2 on page 18 shows the CLYTRAN solution along with the Hanson data. The substep size for 15.77 MeV electrons in gold is 32.08 mg cm² (1.71 × 10⁻³cm) so that the Hanson foil is smaller then the interval substep. Therefore, the entire distribution is calculated in the subroutine ANGLE by the crude approximation. From Figure 2 on page 18 it is shown that this approximation gives a much wider Gaussian width then the experimental data. Figure 3 on page 19 and Figure 4 on page 20 show the corresponding Jordan-Mack and Moliere methods of correction with the Hanson data. Both correction methods show an overall improvement in the angular distribution. It is of no consequence that the two solutions give similar results because they both consist of small angle approximate Gaussian forms. It will be shown later that there are regions where these methods of correction give different results.

The next step was to compare these two correction methods with experimental data of different energies and materials. Only two other experiments for very thin foils could be found, and they were the papers of Kageyama and Mozley. [Ref. 15: p. 348 and, 16: p. 647] The Kageyama experiment was for 1.66 MeV electrons through both copper and lead foils. For this experiment, the low speed of the electrons effectively increased the

Figure 2.   CYLTRAN Solution with Hanson's data for Gold: Angular Spectrum of transmitted electrons for 15.77 MeV incident electrons through a 18.66 mg cm² gold foil.

18

Figure 3. Jordan-Mack Solution with Hanson's data for Gold: Angular Spectrum of transmitted electrons for 15.77 MeV incident electrons through a 18.66 mg cm² gold foil.
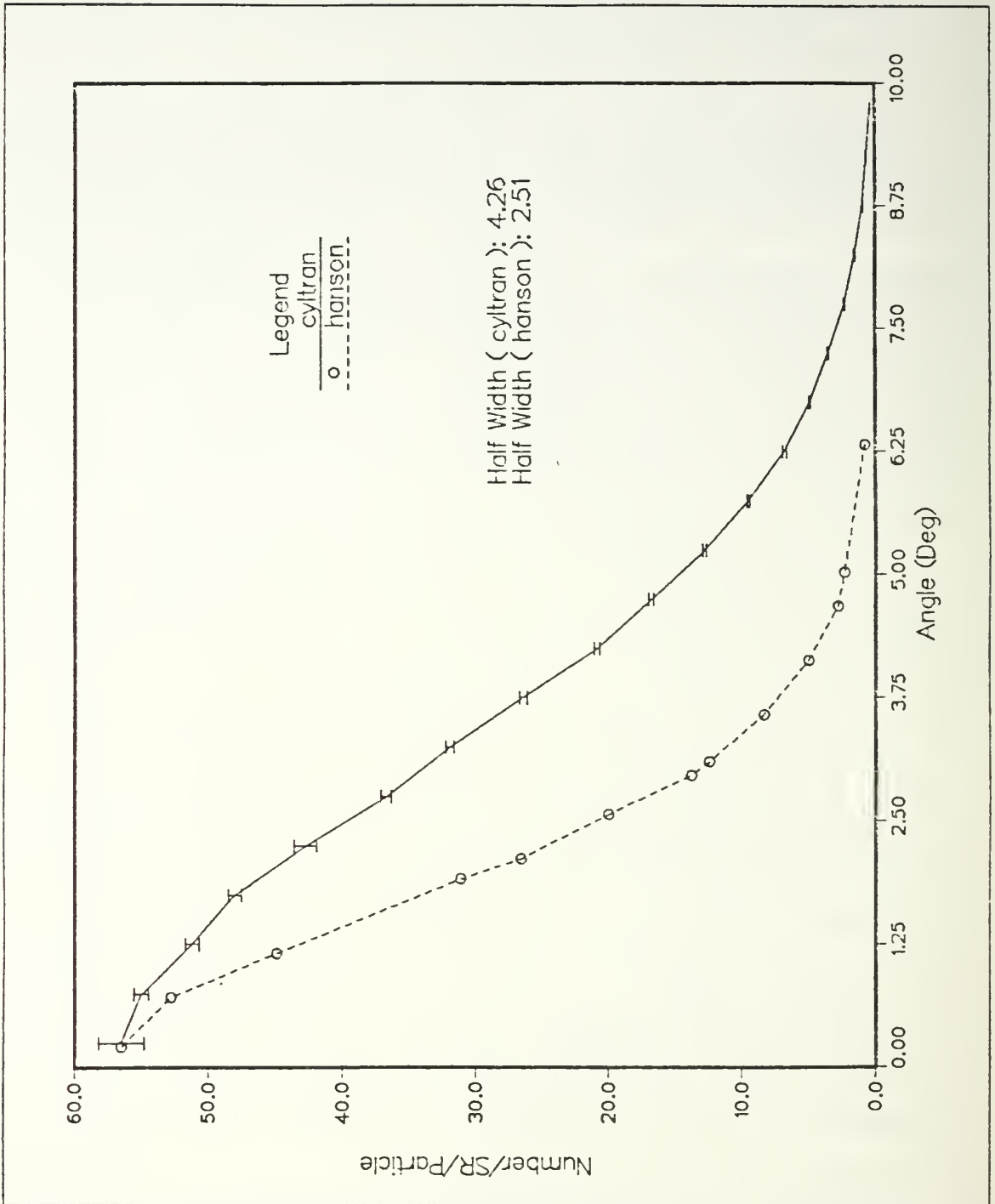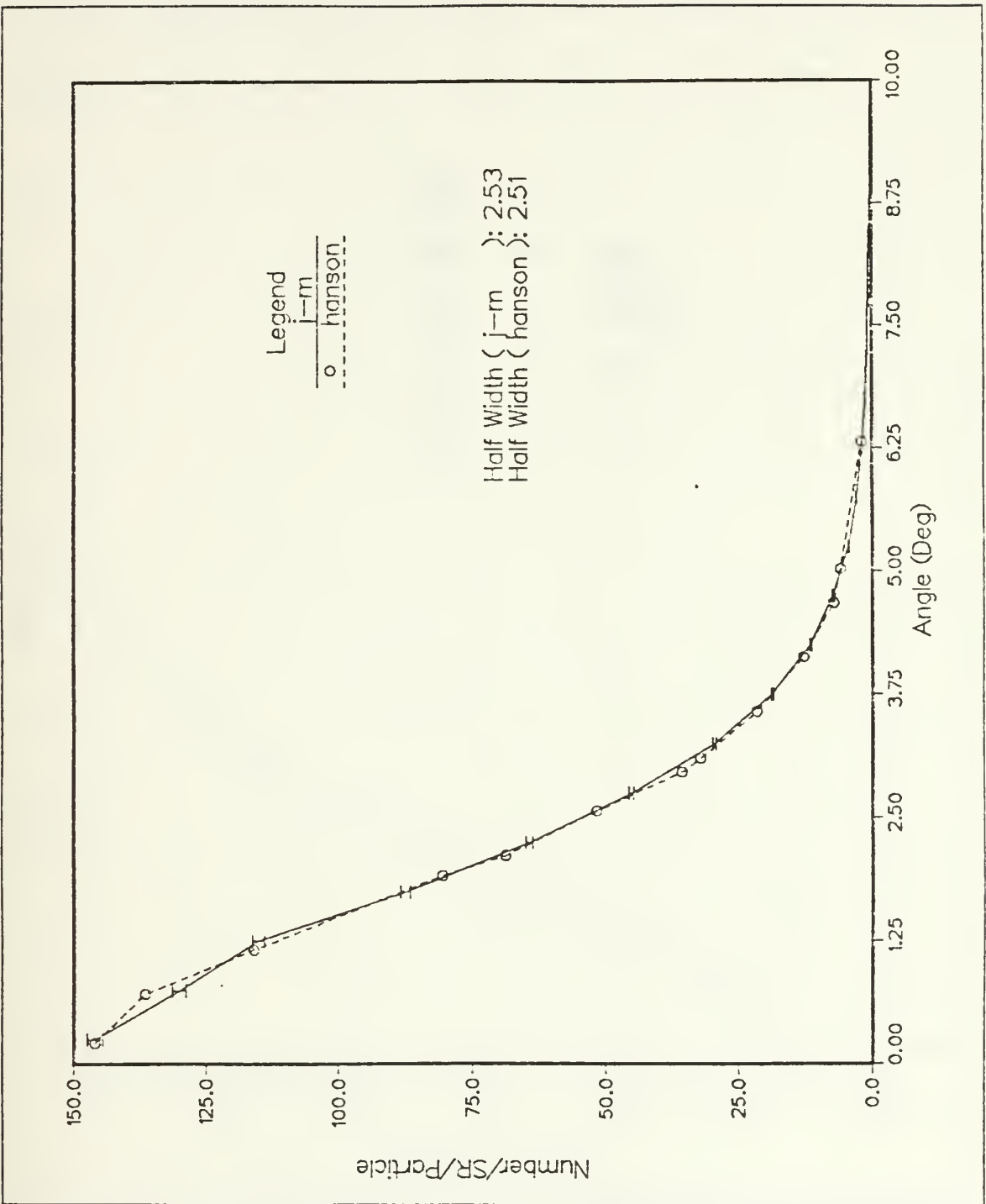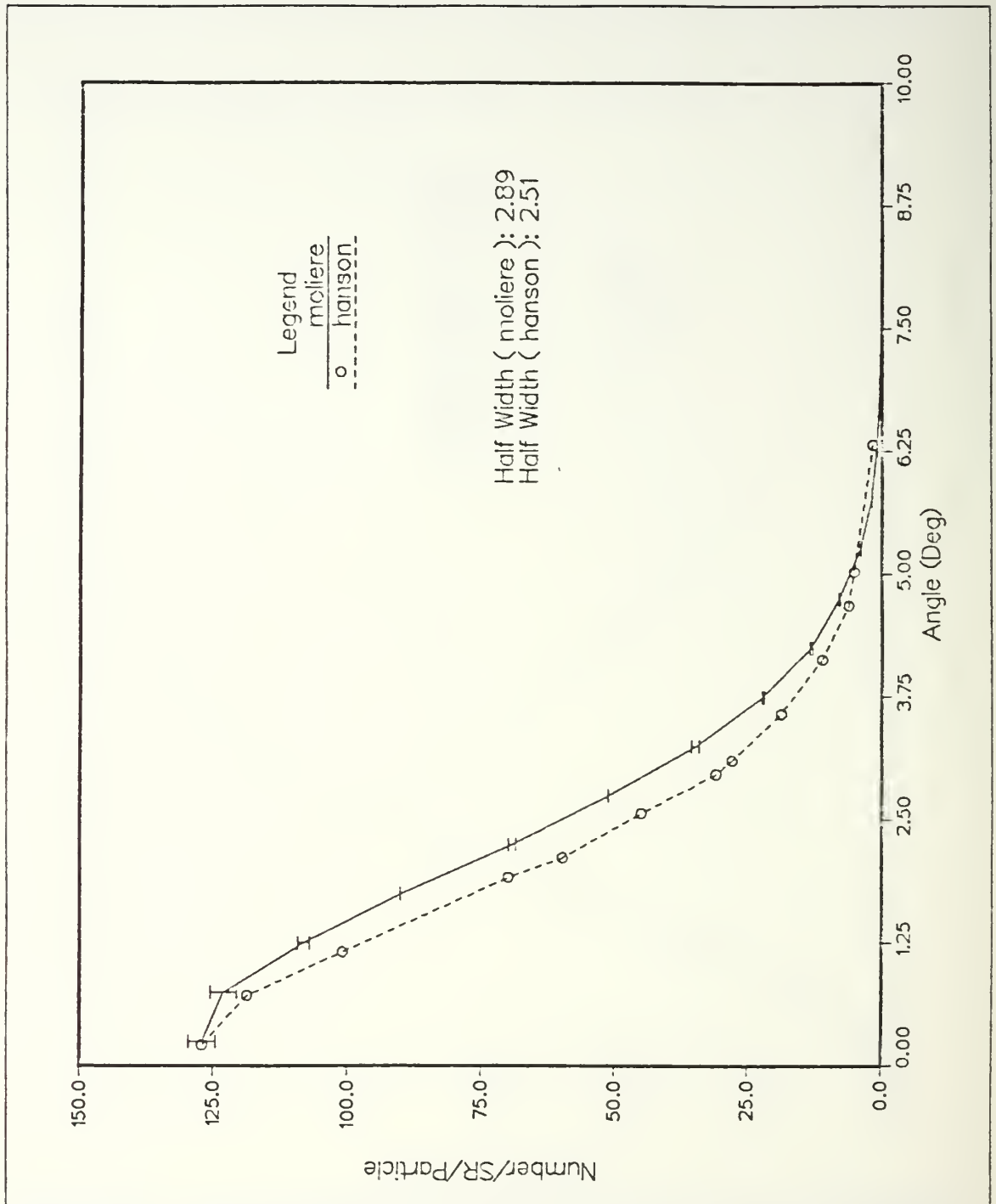
Figure 4. Moliere's Solution with Hanson's data for Gold: Angular Spectrum of transmitted electrons for 15.77 MeV incident electrons through a 18.66 mg cm² gold foil.

number of collisions and a broader Gaussian distribution resulted. The foil thicknesses were 6.3 mg cm² (7.05 × 10⁻⁴cm) and 6.2 mg cm² (5.40 × 10⁻⁴cm) respectfully. The corresponding substep sizes were 14.67 mg cm² (1.64 × 10⁻³cm) and 8.96 mg cm² (7.86 × 10⁻⁴cm). Therefore, the copper foil is thicker then the substep size and is segmented into three substeps. In the first two full substeps, the multiple scattering distribution is calculated by the Goudsmit-Saunderson theory. The third substep is less than the substep size so that the deflection angles are calculated by the approximation in the subroutine ANGLE. On the other hand, the thickness of the lead foil is less then the substep size so that only the ANGLE subroutine is used for the scattering distribution. Figure 5 on page 22 shows the CYLTRAN solution for the copper case, and again the distribution is much broader than the experimental data. The Jordan-Mack method (Figure 6 on page 23), does not show exact agreement as in the Hanson case; however, it does show an overall correction. For this case, the Moliere model (Figure 7 on page 24) showed the closest agreement to the data.

The lead foil solutions, (Figure 8 on page 25 thru Figure 10 on page 27) show the same trend. The CYLTRAN solution is always broader then the experimental data and for low energies, the Moliere method is better than the Jordan-Mack technique.

On the other end of the energy spectrum, the Mozley experiment was at a much higher energy, 600 MeV, and consisted of scattering through very thin aluminum foils (2.44 mg cm², 9.0 × 10⁻⁴cm). For this case the substep size is equal to 3.99 g cm² (1.48 × 10⁻¹cm), so that the foil thickness is much less than the the substep size. At such high energies (600 MeV), the scattering is in the forward direction and not much greater than 0.02 degrees. This makes it very difficult to resolve the scattering and tally the electrons into such small angle bins. Therefore the curves appear crude. Even with double precision, only a bin width of 0.025 degrees was allowed before floating point underflow errors resulted. In spite of these computational problems, the general trends in the solutions can still be seen. In Figure 11 on page 28 the CLYTRAN solution is given for this case, and the poor agreement to experimental data is clearly shown. The Jordan-Mack solution (Figure 12 on page 29) shows great agreement with the data and is superior to the Moliere case (Figure 13 on page 30).

With the JM solution verified over a range of energies and materials, the research effort appeared to be winding down, until something unexpected resulted! When the half width values for several gold foil thickness calculations were plotted for both the CYLTRAN and the JM solutions, a periodic "saw-tooth" pattern resulted (Figure 14 on page 32). Only when the periodicity was determined to be the substep size did this

Figure 5.   CYLTRAN Solution with Kageyama's data for Copper: Angular Spectrum of transmitted electrons for 1.66 MeV incident electrons through a 6.3 mg cm² copper foil.
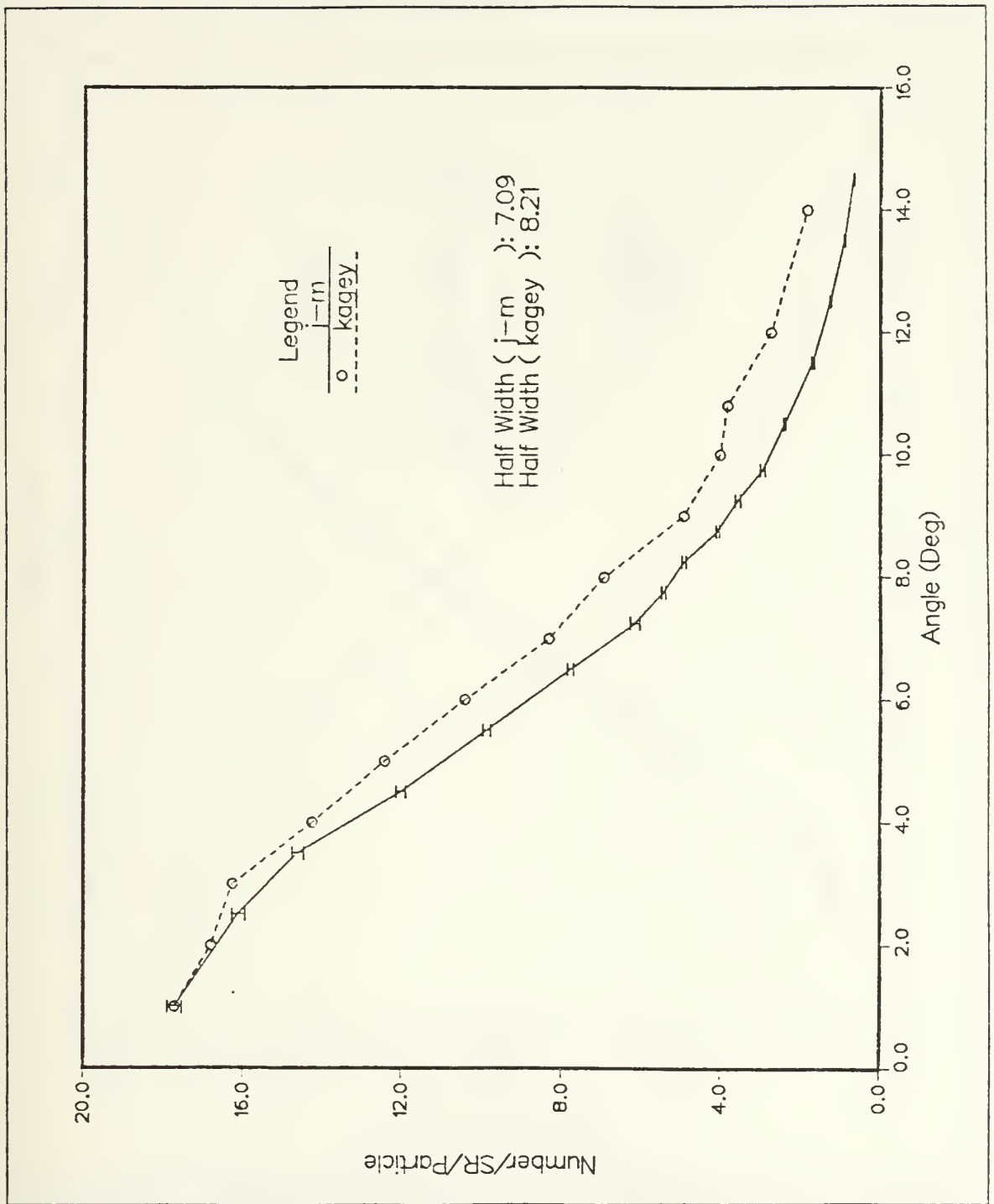
Figure 6. Jordan-Mack's Solution with Kageyama's data for Copper: Angular Spectrum of transmitted electrons for 1.66 MeV incident electrons through a 6.3 mg cm² copper foil.

23
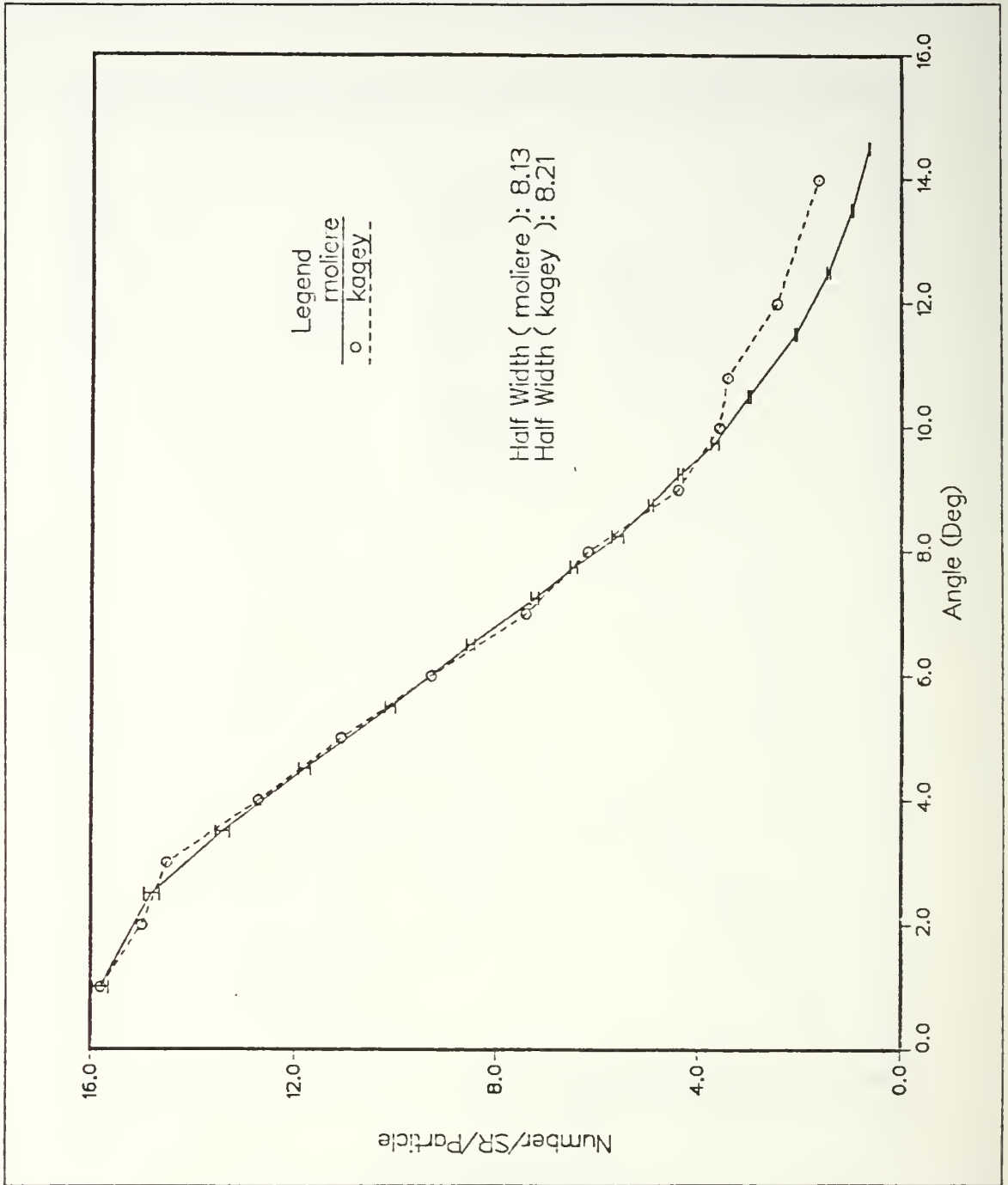
Figure 7.   Moliere's Solution with Kageyama's data for Copper: Angular Spectrum of transmitted electrons for 1.66 MeV incident electrons through a 6.3 mg cm² copper foil.
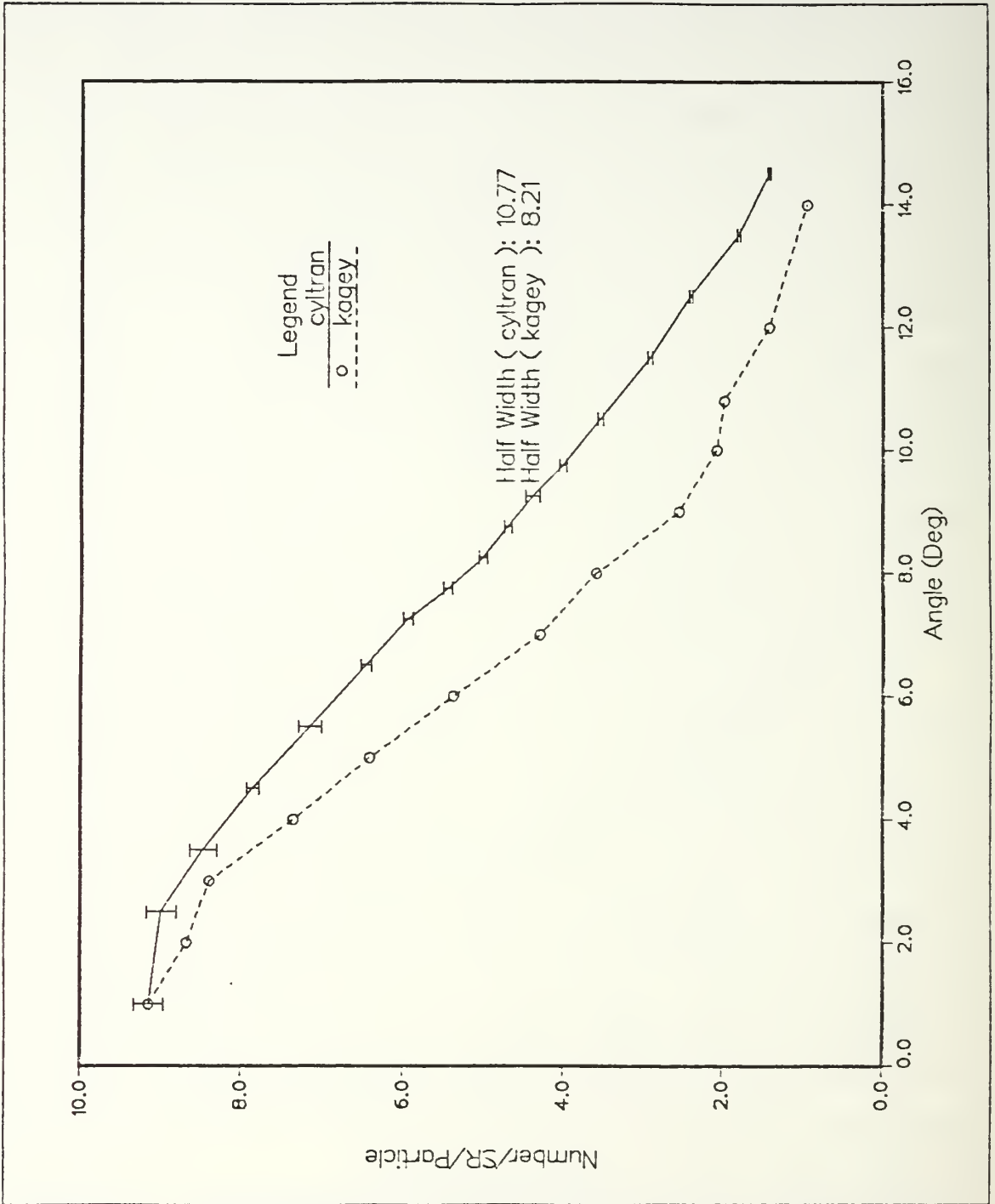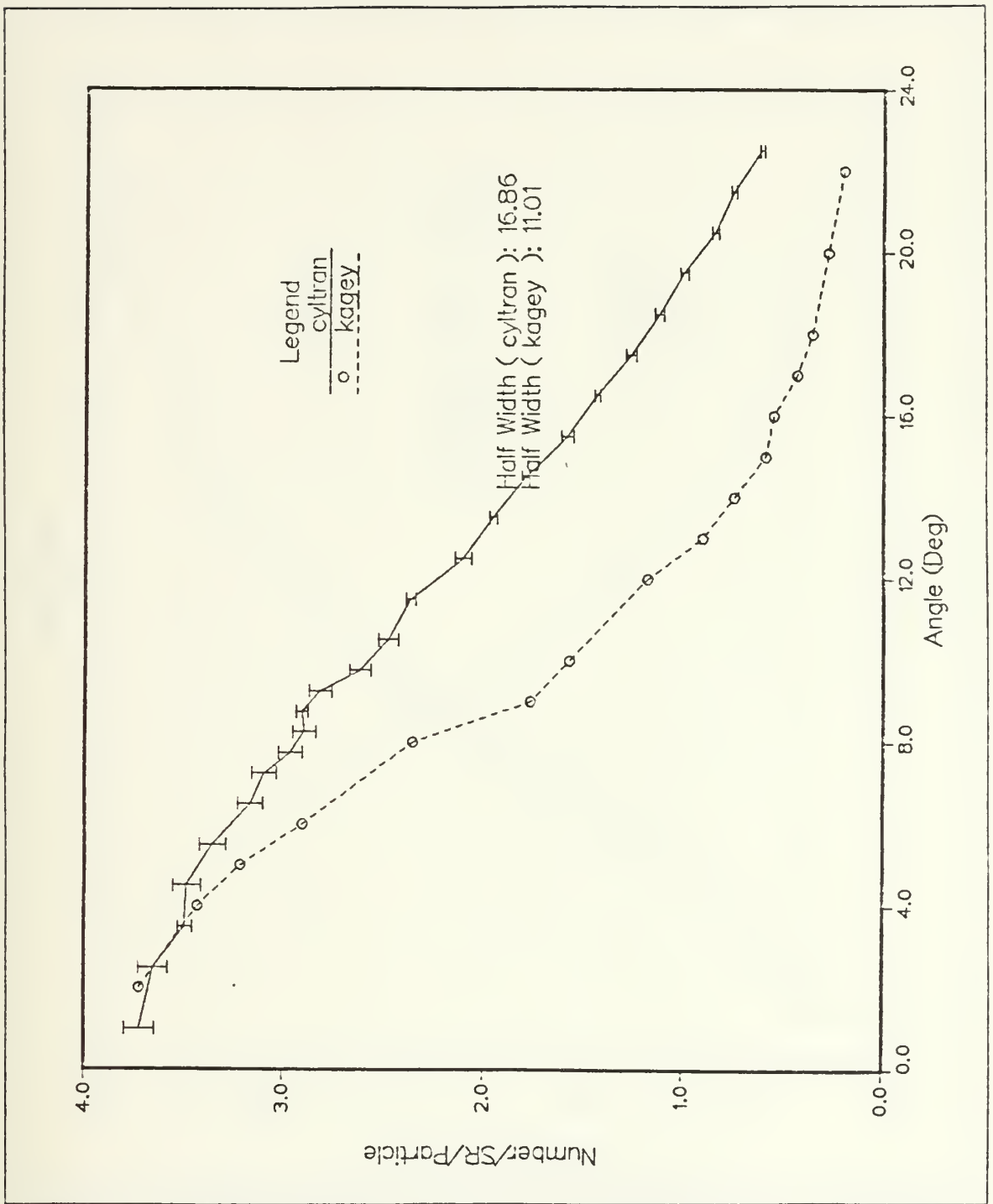
Figure 8. CYLTRAN Solution with Kageyama's data for Lead: Angular Spectrum of transmitted electrons for 1.66 MeV incident electrons through a 6.2 mg cm² lead foil.

Figure 9.   Jordan-Mack's Solution with Kageyama's data for Lead: Angular Spectrum of transmitted electrons for 1.66 MeV incident electrons through a 6.2 mg cm² lead foil.

Figure 10.   Moliere's Solution with Kageyama's data for Lead: Angular Spectrum of transmitted electrons for 1.66 MeV incident electrons through a 6.2 mg cm² lead foil.

Figure 11.   CYLTRAN Solution with Mozley's data for Aluminum: Angular Spectrum of transmitted electrons for 600 MeV incident electrons through a 2.44 mg cm² aluminum foil.

Figure 12. Jordan-Mack's Solution with Mozley's data for Aluminum: Angular Spectrum of transmitted electrons for 600 MeV incident electrons through a 2.44 mg cm² aluminum foil.

29
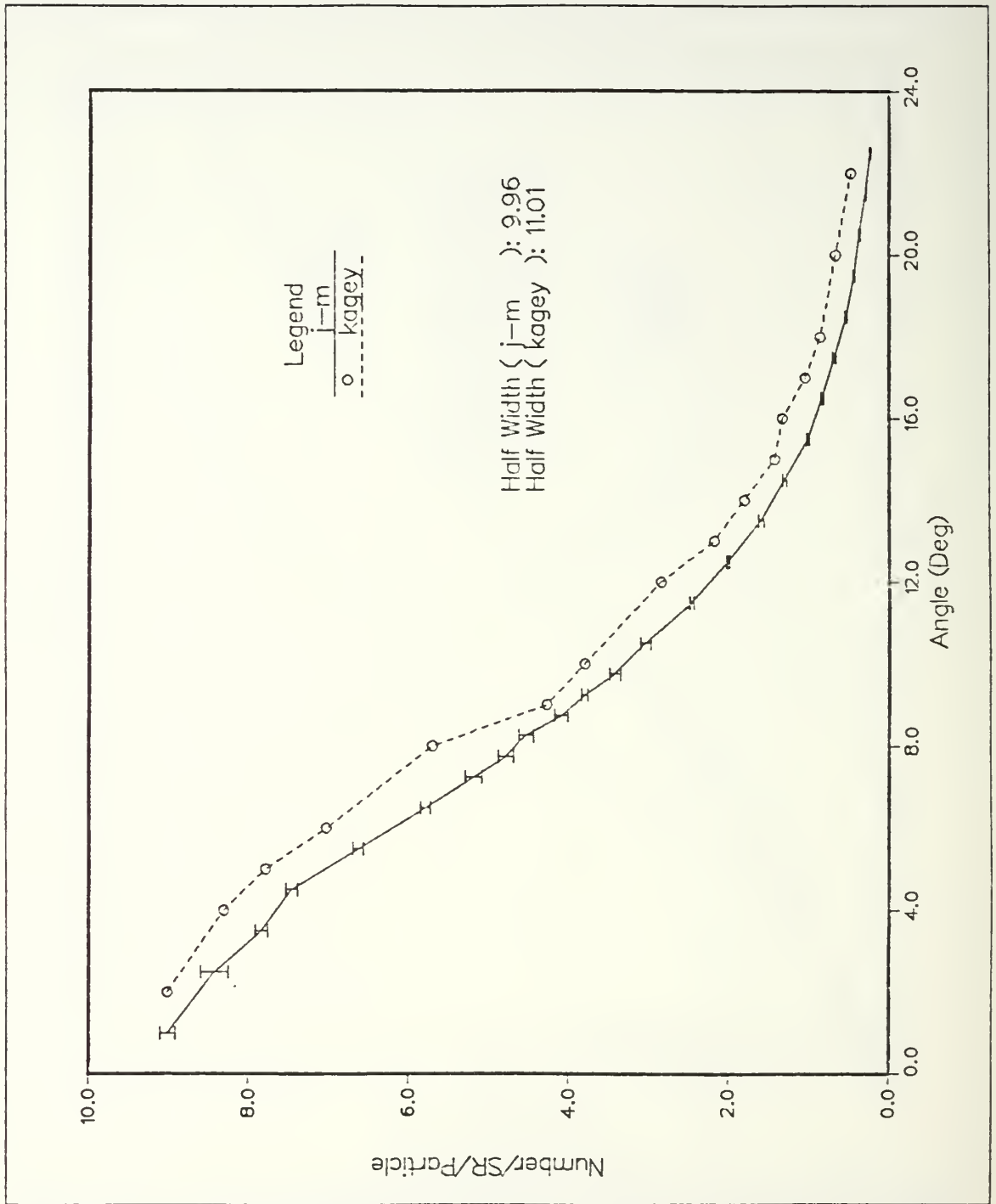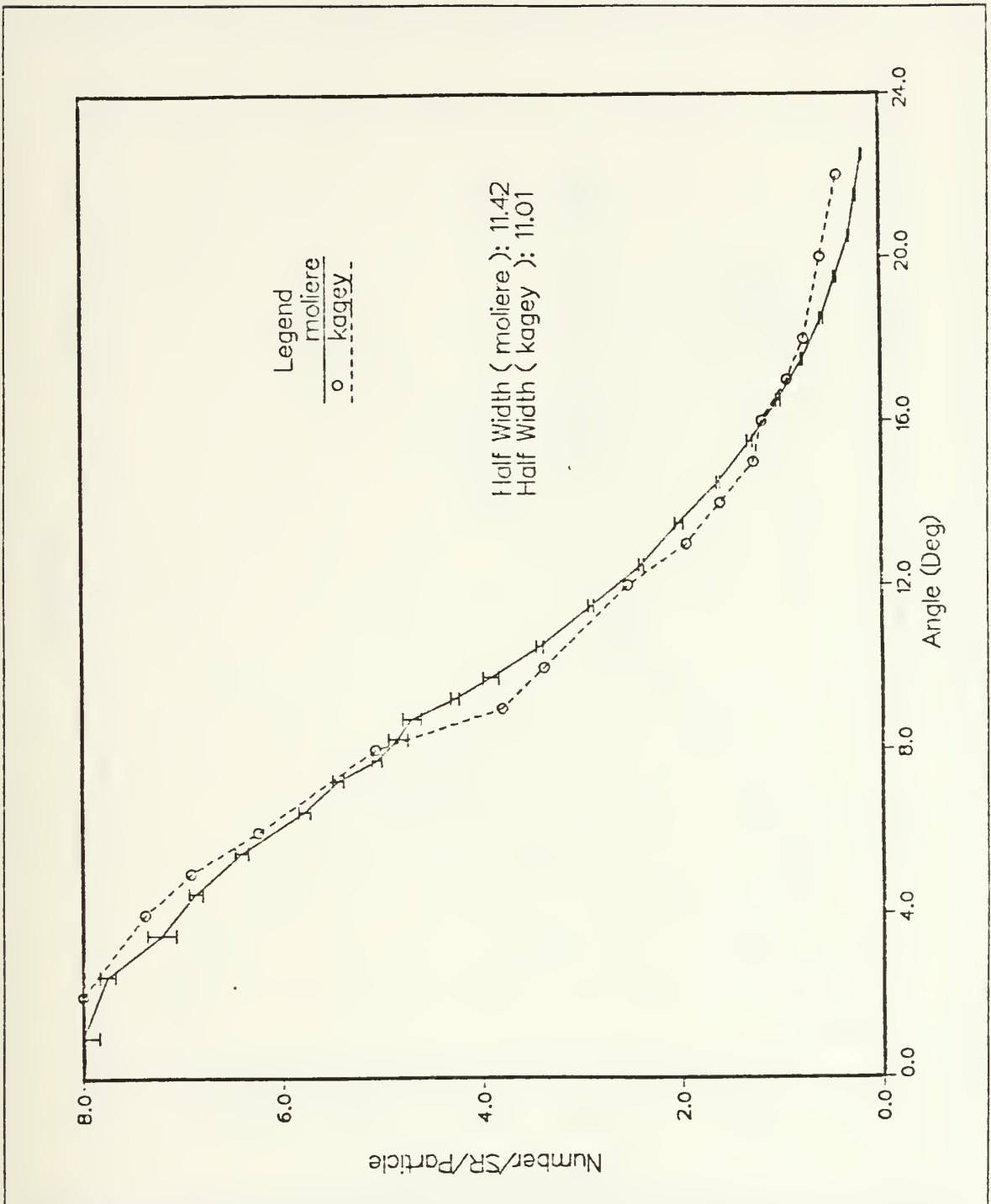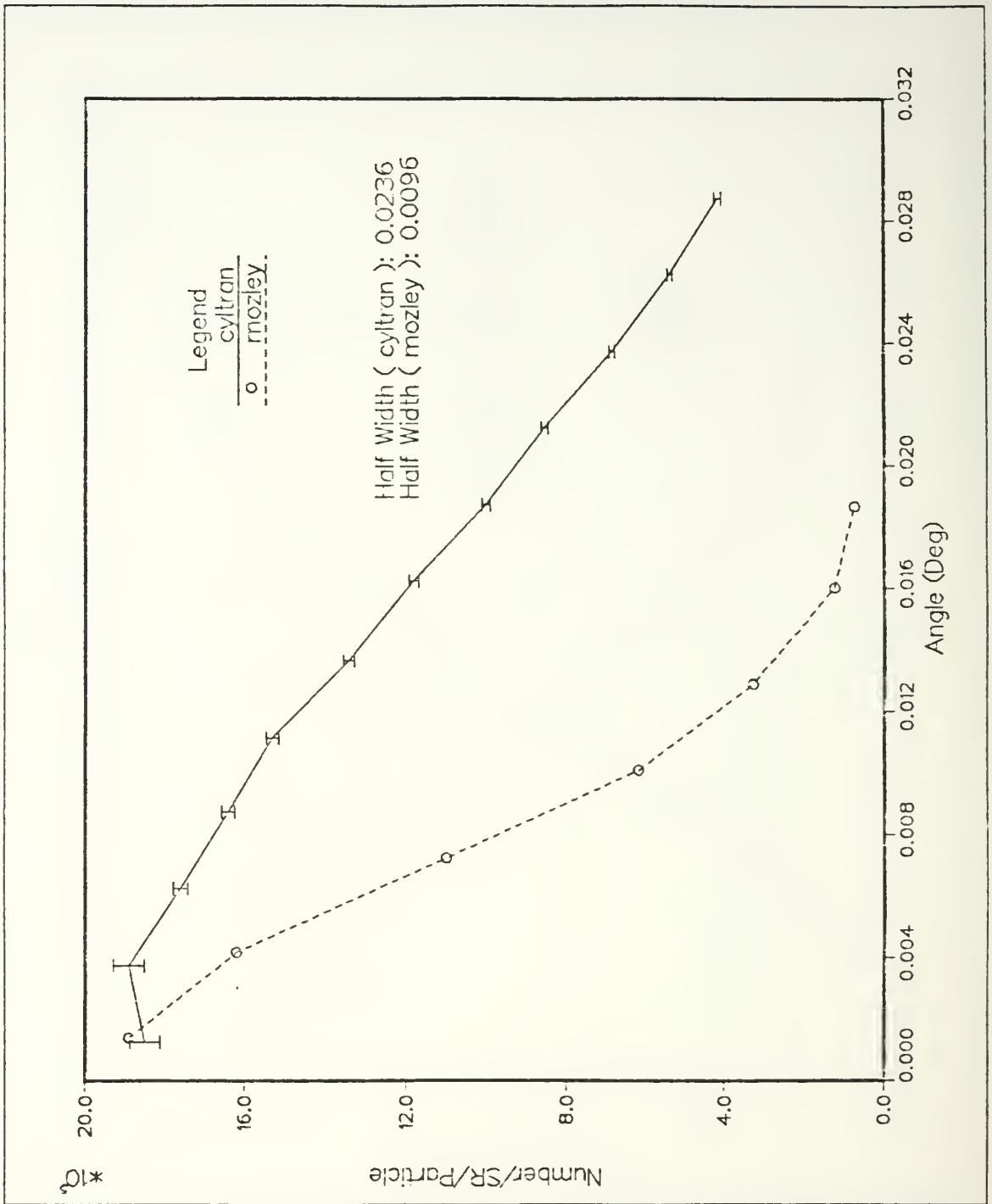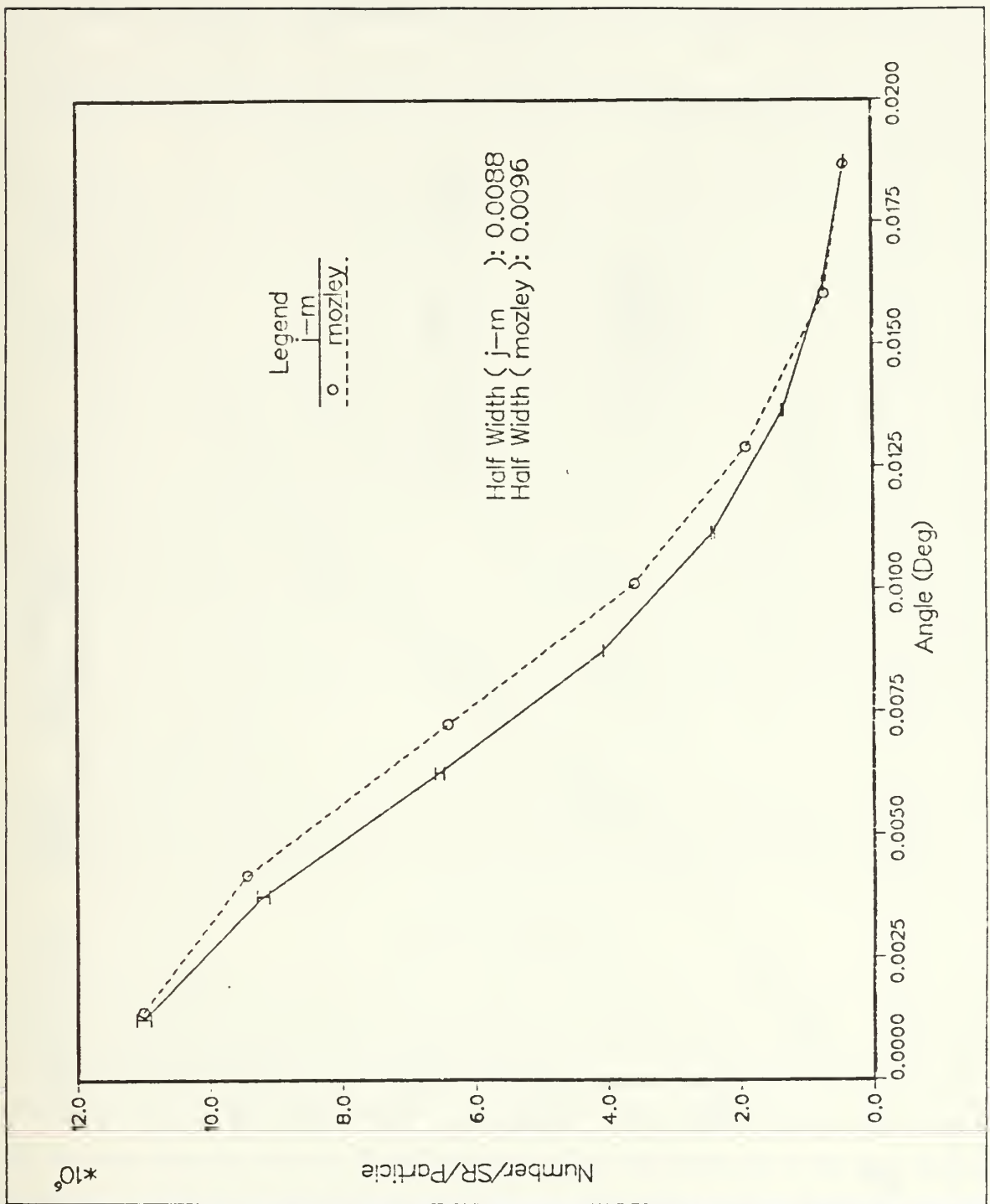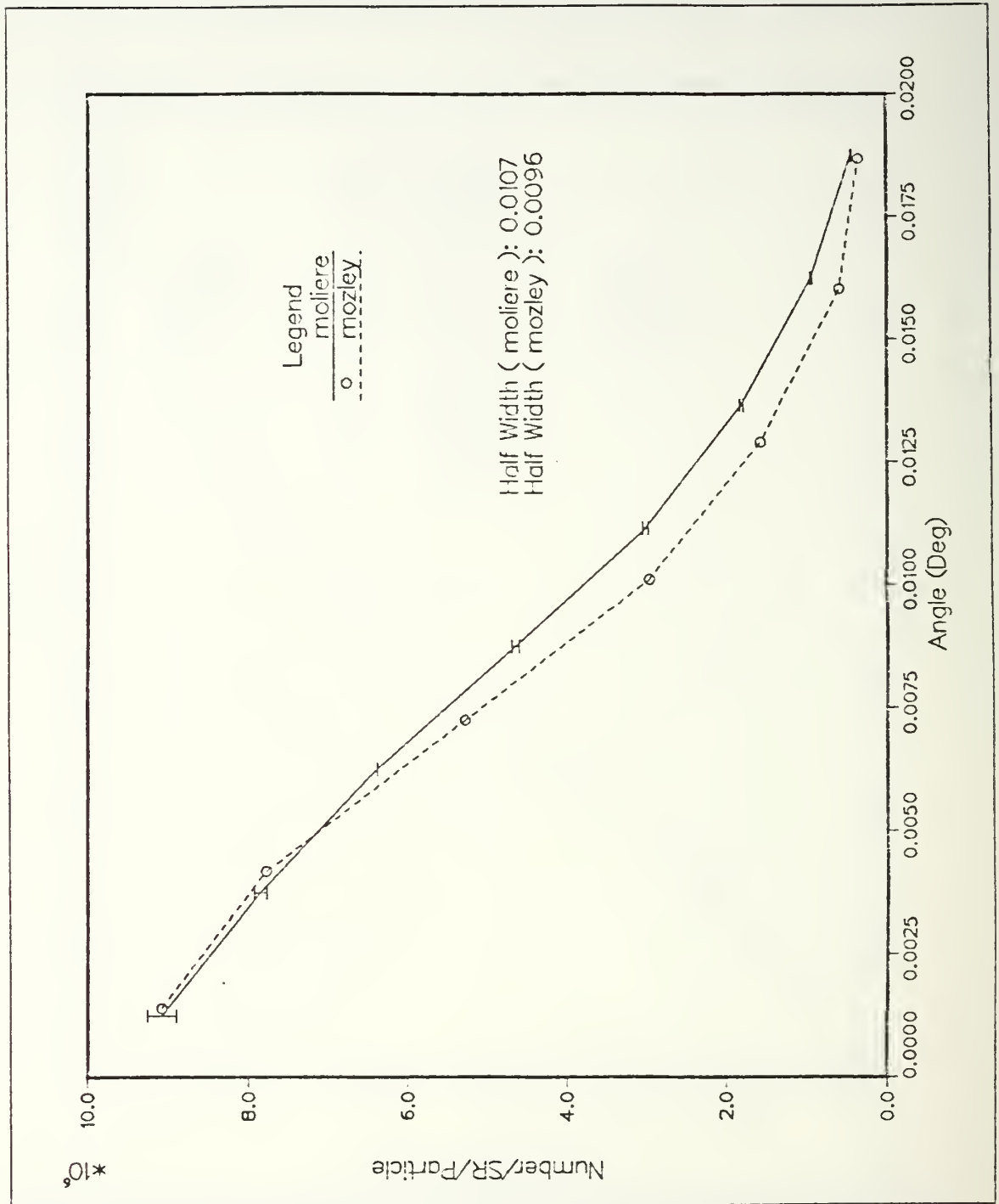
Figure 13.   Moliere's Solution with Mozley's data for Aluminum: Angular Spectrum of transmitted electrons for 600 MeV incident electrons through a 2.44 mg cm² aluminum foil.

pattern make sense. In the original ITS code, the angular distribution within a full substep is calculated by the Goudsmit-Saunderson theory. If the distance between the last full substep and the escaping edge is less than the substep length, the subroutine ANGLE is called to calculated the distribution for the region using the crude approximation. As shown in the theory section, this approximation is dependent on the distance between the last substep boundary and the escaping edge. The larger this distance is, the larger the error in the approximation will be. However, if the foil thickness is exactly equal to the substep size, or a multiple of this size, the entire distribution will be calculated by the Goudsmit-Saunderson theory and the subroutine ANGLE will never be called. The effect is such that the error from the approximation grows until the distance between the last substep and the edge is equal to a substep and then the solution "corrects" itself by a Goudsmit-Saunderson calculation. With this explanation, a better understanding of the subroutine ANGLE is given. For the existing ITS material interface approximation there is a strong dependence on the foil thickness. On the other hand, the Jordan-Mack method shows very little dependence on this distance parameter SHD. For very thick foils the error of approximation at the escaping edge is a small fraction of the total distribution which has already been established by the multiple substep GS calculations within the material. A semi-log plot shows this graphically (Figure 15 on page 33).

An interesting result of the Jordan-Mack solution is the apparent evaluation of Moliere's iteration B_m. Upon comparison of the two forms of the Gaussian distribution, (equations (3.27) and (5.9)), a Jordan-Mack constant can be formed and is given by:

$$B_{jm} = \chi_d^2 - \ln(\chi_d^2) - 1$$

Comparisons of B_m and B_{jm} are shown in Figure 16 on page 34 and Figure 17 on page 35. In Figure 16 the energy is held constant at 15.77 MeV, while the foil thickness is varied from 10 microns to one meter. This figure shows the region where the Jordan-Mack solution and the Moliere theory give similar results. At around eight centimeters B_{jm} becomes constant whereas B_m still increases. Since the thickness of the final partial substep is usually much less than a centimeter this region is of little concern. Figure 17 on page 35 however does contain an important result. In Figure 17 on page 35, the foil thickness is held constant and the incident electron energy is varied from one electron volt to several MeV. Again there is a region where the two theories are similar. At around 0.5 MeV the two iterative constants level off, but for energies less than this, the
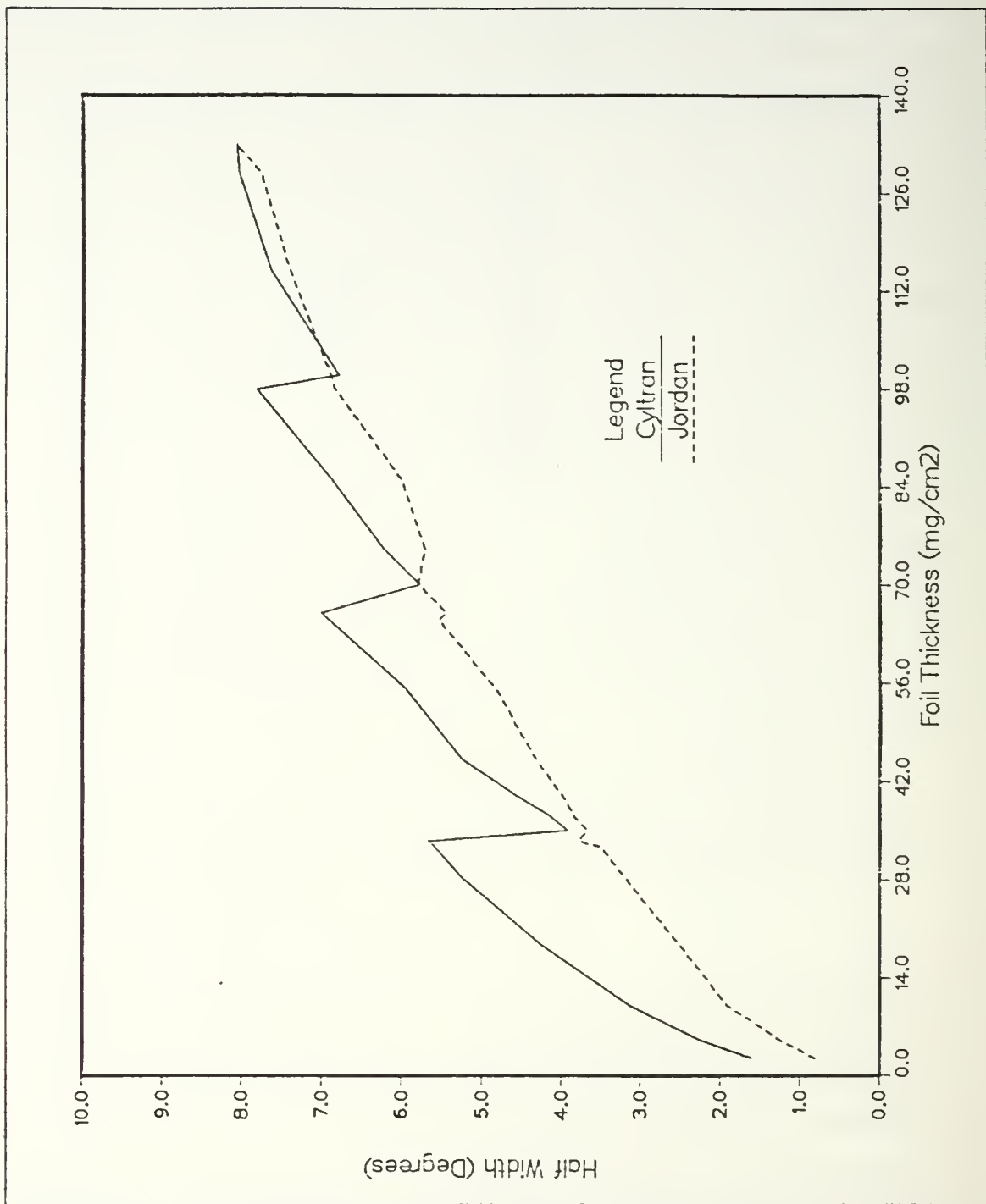
Figure 14.   Half Widths (CYLTRAN with Jordan-Mack; Linear):   The input
parameters were for 15.77 Mev incident electrons through gold foils of
various thickness.
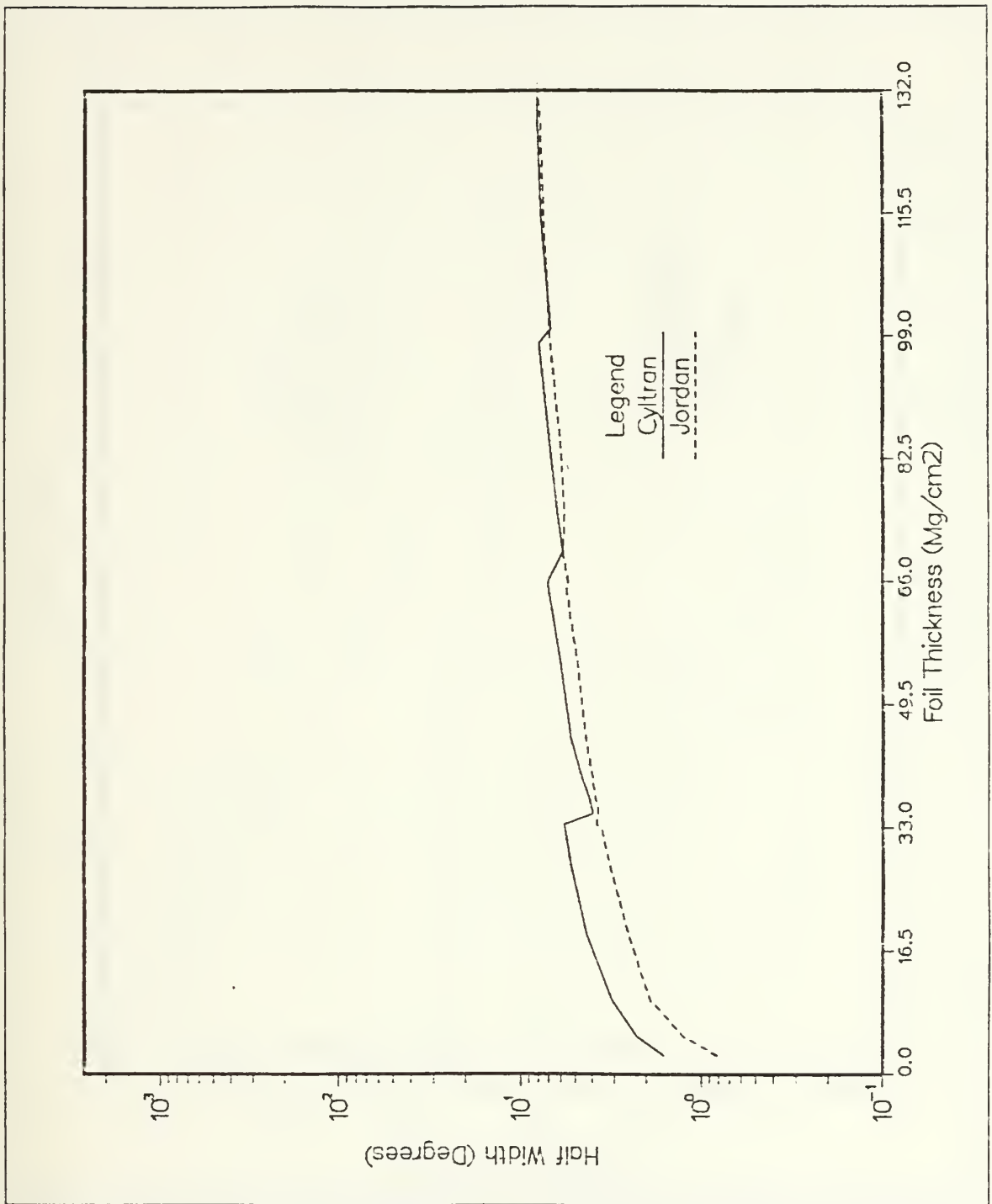
Figure 15. Half Widths (CYLTRAN with Jordan-Mack; Semi-Log): The input parameters were same as Figure 14 on page 32
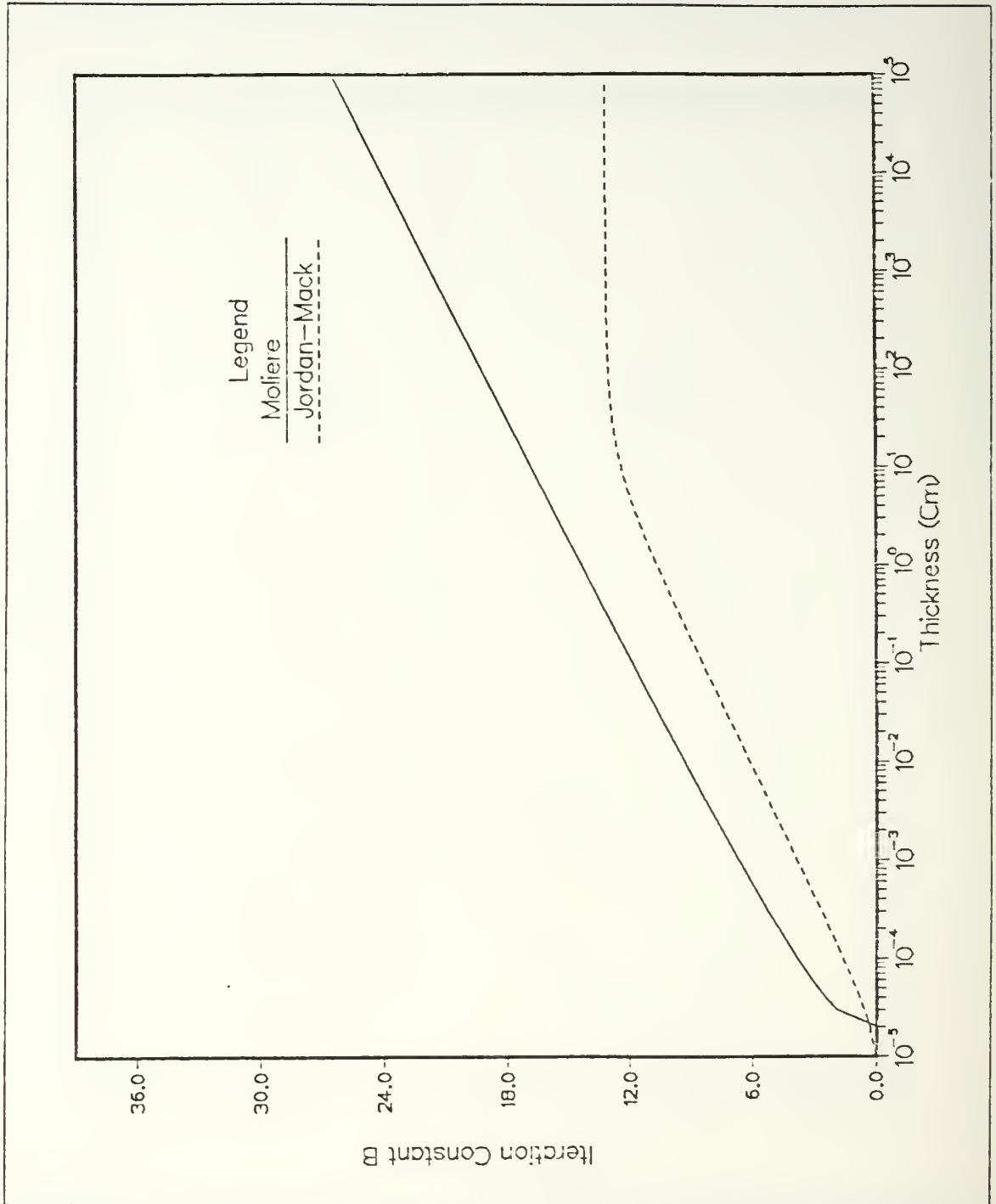
Figure 16.   Iterative Constant Comparison (Moliere with Jordan-Mack):   The input parameters were for 15.77 MeV electrons through gold foils of varying thickness.
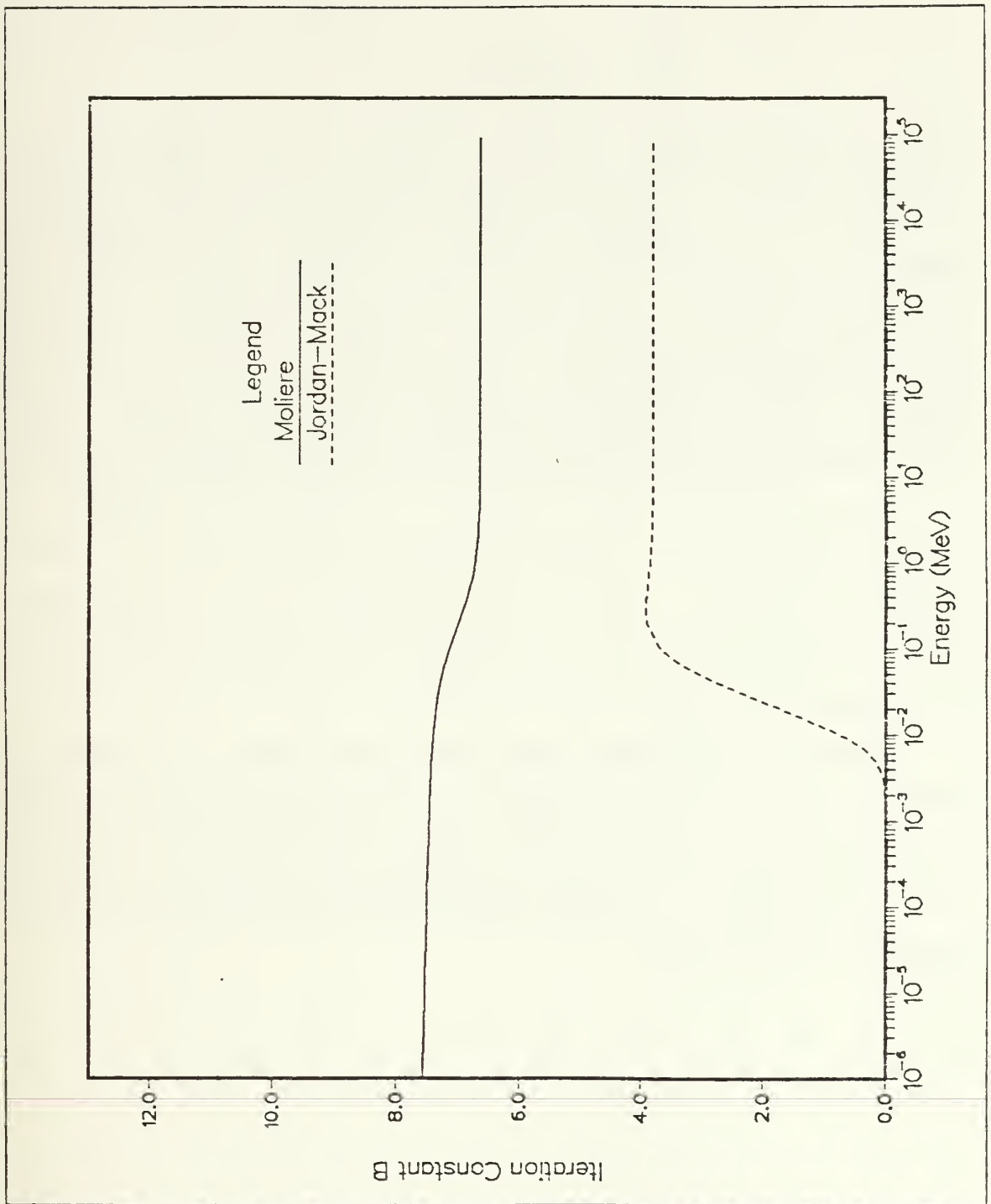
Figure 17.   Iterative Constant Comparison (Moliere with Jordan-Mack):   The
input parameters were for a 18.66 mg cm² gold foil with incident
electrons of varying energy.

35

two curves diverge. Recall that this iterative constant B is a measure of the Gaussian width of the scattered distribution. Since B is in the denominator of the exponential, when B increases the width of the distribution increases. Physically, when the incident electron energies are low the number of collisions should increase and the Gaussian width of the distribution should increase. Therefore the value of B should increase as the energy decreases. The Jordan-Mack solution appears to break down at energies less than 0.5 MeV. To investigate this problem a "stand-alone" fortran program named JORDAN was utilized. JORDAN is simply a bin tally program which uses the Jordan-Mack correction scheme to form the cumulative distribution function from which the incident electron angle deflections are drawn. In addition to the standard transmitted electron distribution, program JORDAN gives the distributions of both the small and large angle scattering. The program is given in Appendix D. With the "stand-alone" program several problem runs could be quickly conducted at many different energies. The results of those runs are given in graphical form in Appendix E. For the small angle distribution a discontinuity developed at energies less than 0.5 MeV at an angle of 105 degrees. At 0.01 MeV this discontinutity grows into a major peak. In this case the small angle distribution has been extended far beyond it's region of validity. We must remember that small angle approximations were used in the developement of the distribution equations.

The large angle distributions for the related energies show the same pattern. For energies less than 0.5 MeV the discontinutity at 105 degrees becomes large. One explanation is that the large angle scattering in the Jordan-Mack correction is based on a Possion distribution which requires the probability of a single event to be very small. As the energy decreases, the number of large angle scatters becomes large and Poisson statistics are not applicable.

VI. REMARKS

This study looks only at the angular distribution of the transmitted electrons. Although the energy deposition for very thin foils is small, this aspect of the code and the correction should be investigated. Another of area of interest which needs elaboration is the apparent discontinuity in the small and large angle distributions at energies below 0.5 MeV. The problem occurs at 105 degrees and is not Z dependent (See Appendix E). Finally, all the comparisons for this study were calculated using ITS version 2.0. An updated version 2.1 has recently been installed at the Naval Post Graduate School. Trial runs have shown the same problems in regard to very thin foils. Version 2.1 contains a correction to the Landau Straggling Algorithm and doesn't effect the subroutine ANGLE. [Ref. 17]

VII. CONCLUSIONS

The existing CLYTRAN code approximation for the multiple scattering in very thin materials is inadequate when the thickness of the foil is less then three substep intervals. The Jordan-Mack correction shows an improvement over a wide range of energies and materials. The Jordan-Mack scheme does however break down for very thin materials when the energy of the incident electron beam is less than 0.5 MeV. For moderate energies the Jordan-Mack method gives better results then the Moliere first term approximation. Of course if more Moliere terms were used this difference would be minor. In addition, is was shown that although the large angle scattering distribution makes a small contribution, it should not be ignored for moderate energies. Future versions of the ITS code system should include a correction to the multiple scattering for very thin materials. Finally, the range of applicability must be determined and documented with the final version.

APPENDIX A.   ITS OVERVIEW

The Integrated Tiger Series of Electron Photon Transport codes (ITS) is the most widely used particle transport code in the world. The code package was developed to incorporate eight individual codes which were developed over the period from 1968 to 1981. All the codes are based on the original ETRAN model developed by M. Berger and S. Seltzer. The ITS code system consists of four primary code packages [Ref. 1: p. 9]:

XDATA: The electron and photon cross section data file.

XGEN: The cross section generation program.

ITS: The Monte Carlo program file.

UPEML: A machine portable update emulator.

The heart of the ITS is the program library file ITS, which contains the eight Monte Carlo programs plus system directives for the CRAY, IBM, VAX, and CDC operating systems. The update emulator program UPEML creates the various Monte Carlo codes for a given system with any corrections to those codes that may be desired. The output fortran source code from UPEML is then compiled and stored as an executable module. Program XGEN generates the problem specific cross section data tape using file XDATA for referenced inputs and a user defined input file. The Monte Carlo codes then read in the cross section tape and process the user defined problem.

One of the eight ITS codes is CYLTRAN, which simulates the transport of particle trajectories through a three-dimensional multimaterial cylinder. For this project only the CYLTRAN code was required. As an ITS user the following steps were required to execute an ITS run

1. Create the specific ITS code CYLTRAN with the required correction schemes.

2. Generate a cross section tape based on the different type of materials contained in the cylindrical geometry of a problem.

3. Create an input file which list all the input parameters required to calculate desired outputs.

4. Submit the input file and the generated cross section tape to the ITS Monte Carlo codes to execute a run.

Table 1 is a sample input file to generate the cross section tape for the materials in a cylindrical geometry. Each material line represents a different medium in the cylinder. Percentages of each material in a compound and its density must be specified. Single element lines such as Cu, has its density stored in ITS and is automatically used for the simulation when needed.

Table 1. SAMPLE INPUT FILE TO CREATE A CROSS SECTION TAPE

```
Energy 16.0
Material Cu
TITLE
     16 MeV Cross Section for Au foil
```

Once a cross section tape is generated, an input file with the parameters design for a particular simulation must be created. Table 2 on page 41 is a sample input file to execute an ITS run. The keywords at the beginning of each line are relatively self-explanatory. However, a few keywords and their numerical parameters require some explanation to fully understand their importance. These few keywords and their explanation are listed [Ref. 1: pp. 21-23]:

Geometry This keyword sets up the cylindrical geometry of the problem into input zones, where in this case there are seven input zones. Each line of numerical parameters following the keyword describes the dimensions of each zone.

Electron/Photon-Escape This keyword tallies the number of incident electrons and photons that escapes the cylindrical geometry, either latterally or transmitted through.

NBINE tallies the escaped electron photons in specified energy bins.

NBINT tallies them in angular bins.

Electron/Photon-Flux This keyword tallies the energy deposition of electrons and photons in the subzones described in the keyword geometry.

Histories This keyword represents the number of primary particle histories to follow as it transport through each medium in the cylinder.

Table 2.   SAMPLE OF AN INPUT FILE TO EXECUTE ITS

```
Echo 1
TITLE
   Mat:Au 18.67 Mg/cm2 His:100000 E = 15.77MeV
Electrons
Energy 79.0
Cutoffs .1 .1
Position 0.0 0.0 0.0
Direction 0.0 0.0
Geometry 1
      0.000       0.00096684 0.00       10.000      1    0    1    1
Electron-Escape
   NBINT 24 User
      0.5 1. 1.5 2. 2.5 3. 3.5 4. 4.5 6. 6.5 7.
      7.5 8. 8.5 9. 9.5 10. 15. 45. 90. 180.
   NBINE 1 User
      0.1
Histories 100000
```

41

APPENDIX B.   JORDAN-MACK EQUATIONS

The Jordan-Mack correction to the multiple scattering for very thin foils is based on a Williams Gaussian distribution. To determine the mean square angle, the screened Rutherford cross section with Moliere's screening angle are combined and integrated over the forward region:

$$\omega^2 = Nt \int_0^{\theta_m} \theta^2 \, d\sigma \tag{B.1}$$

$$\omega^2 = Nt \int_0^{\theta_m} \frac{2\pi e^4 Z^2}{p^2 v^2} \frac{2(1 - \cos\theta)}{(1 - \cos\theta + \eta)^2} \, d(\cos\theta) \tag{B.2}$$

where $\eta = {}^1\!_2\theta_1^2$ is one half the value of Moliere's screening angle and the small angle approximation of $\theta^2 = 2(1 - \cos\theta)$ has been used. The constants in this integral form the Moliere unit probability angle, and with the substitutions $\mu = \cos\theta \wedge \mu_m = \cos\theta_m$, this equation simplifies into a form which is easy to integrate:

$$\omega^2 = -\chi_c^2 \int_1^{\mu_m} \frac{1 - \mu}{(1 - \mu + \eta)^2} \, d\mu \tag{B.3}$$

$$\omega^2 = -\chi_c^2 \int_1^{\mu_m} \left[\frac{1}{(1 - \mu + \eta)} - \frac{\eta}{(1 - \mu + \eta)^2} \right] d\mu \tag{B.4}$$

$$\omega^2 = -\chi_c^2 \left[\ln(\eta) - \ln(1 - \mu_m + \eta) - \frac{\eta}{1 - \mu_m + \eta} + 1 \right] \tag{B.4}$$

42

This expression can further be simplified by the introduction of the constant χ_d^2:

$$\chi_d^2 = \frac{\eta}{1 - \mu_m + \eta} \tag{B.5}$$

$$\omega^2 = \chi_c^2[\chi_d^2 - \ln \chi_d^2 - 1] \tag{B.6}$$

which is the form given in the theory section. To evaluate the "argument" $(1 - \mu_m + \eta)$, the condition of one scatter occurring in the back region is imposed in the following form:

$$\int_{\theta_m}^{\pi} d\sigma = 1 \tag{B.7}$$

$$-\tfrac{1}{2}\chi_c^2 \int_{\mu_m}^{-1} \frac{1}{(1 - \mu + \eta)^2} \, d\mu = 1 \tag{B.8}$$

$$-\tfrac{1}{2}\chi_c^2 \left[\frac{1}{2 + \eta} - \frac{1}{1 - \mu_m + \eta} \right] = 1 \tag{B.9}$$

Rearranging yields:

$$(1 - \mu_m - \eta) = \frac{1}{\left[\dfrac{2}{\chi_c^2} + \dfrac{1}{2 + \eta} \right]} \tag{B.10}$$

43

APPENDIX C.   FORTRAN SUBROUTINES

A.   ANGLE SUBROUTINE

In the existing ITS code CYLTRAN, the multiple scattering distribution near the escaping boundary is calculated in a subroutine called ANGLE. As described in the theory section, this subroutine uses a Williams-type Gaussian approximation. In a subroutine called XINPUT, the GS average cosines with the corresponding D ranges are read from the cross section tape and stored in the variable names COSAV and DRG. In the subroutine XPREP the variable name COSAV is transformed into a proportionality constant by the following code:

```
DRGS(N,J)  = DRG(N,J)/ISUB
COSAV(N,J) = ( CONE-COSAV(N,J))/DRGS(N,J)XPREP
```

where ISUB is the number of substeps and CONE is the constant one. Since the D ranges are in units of Mg cm^2 this proportionality constant is then multiplied by the density in a subroutine called PREP so that the COSAV values are ready for the AN-GLE subroutine. The crude approximation is done in only nine lines of code. When the proportionality terms COSAV are multiplied by the distance to the edge boundary, SHD, the resulting term represents an approximation to the average cosine of the deflection angle for that specific distance:

```
ALF = COSAV(NT,MT)*SHD
RA = RAN(IRAN)
IF (RA .LT. C1EM2) THEN
     ARG = MAX(-C88,-CTWO/ALF)
     EX  = EXP(ARG)
     COM = CONE+ALF*LOG(RA*(CONE-EX)+EX)
ELSE
     COM = CONE+ALF*LOG(RA)
ENDIF
```

The constants CONE, CTWO, C1EM2, and C88 are the values 1.0, 2.0, 0.002, and 88.0 respectively.

The expression for the cosine of the deflected angle COM is derived from the Williams Gaussian expression which is formed into a CDF and from which a random value is drawn:

$$\exp\left[-\frac{\theta^2}{\theta_m^2}\right] = \exp\left[-\frac{2(1-\cos\theta)}{2(1-\cos\theta_m)}\right] \qquad (C.1)$$

$$\exp\left[-\frac{\theta^2}{\theta_m^2}\right] = \exp\left[\frac{(1-COM)}{ALF}\right] \qquad (C.2)$$

B. ANGDET SUBROUTINE (JORDAN-MACK METHOD)

For the Jordan-Mack correction scheme a subroutine called ANGDET was developed to be called from the ITS subroutine ANGLE. All the previous coding just described for the crude approximation was deleted by the following code:

```
*DELETE ANGLE .XX-XX
```

The call statement is then placed in the subroutine ANGLE with the patch subroutine ANGDET placed at the end of ANGLE:

```
*INSERT ANGLE.99
      COMMON/TEMP/JSUB,LMAT(INMT),MPAIR,MTAX(15),NTAB,WT(INEM,INMT),
     1ATW(INEM,INMT).ZE(INEM,INMT)
*INSERT ANGLE.120
C-----------------------------
C  ANGLE DETERMINATION PATCH  C
C-----------------------------
      CALL ANGDET(COM,SHD,T,RHO(MT),ZE(1,MT),ATW(1,MT))
C
C-----------END OF PATCH------C
*INSERT ANGLE.190
      SUBROUTINE ANGDET(COM,SHD,E,RHO,Z,A)
      DOUBLE PRECISION COM,STH,CTH,SPH,CPH,ETA,FST,HST,AST,
     1 BST,XMP,P1,THE2,TARG,SARG,THE,ROT.PEXP,ALXMP,POFN
      DOUBLE PRECISION R,RX,RF,RARG,ARG,COSMAX,POF,POFZ,XTON
      DOUBLE PRECISION DSEED,IRAN
      COMMON /VAXRAN/ IRAN
      DIMENSION ROT(3,3),R(3,3),RX(3,3)
      DATA PI,RZERO,EMZERO,ALPHA,AVA/3.1415926536D00,0.281751
     1,0.511,137.0371,0.6025/
      RAN(DSEED)=GGUBFS(DSEED)

   Initialization of the Constants:

      ET=E/EMZERO + 1.
      B21= 1./(ET*ET)
```

```
      B2= 1. -B21
      Z3= Z**.333333
      ETA = .5*(B21/B2)*(Z3/(.885*ALPHA))**2
    1 *(1.13 + 3.76*(Z/ALPHA)**2/B2)
      FST = 2.*PI*RZERO**2 *Z*(Z+1) *B21/(B2*B2)
    1 *(AVA/A)*SHD*RHO

   Determination of the Integral Values:

      HST = 1.+ETA
      AST = 1./(HST+1.0)
      RARG = 1./FST + 1./(2.+ETA)
      ARG = 1./RARG
      COSMAX = HST - ARG

   COSMAX is the maximum angle such that one large angle scatter will
         occur in the back region.

  144 IF (COSMAX.LT.1.) GOTO 10

   When COSMAX is greater than one, a large angle scatter is not
   possible so that an explicit angle determination must be carried out.

      COSMAX = 1.0
      BST = 1./ETA -AST
      XMP = FST*BST
      COM = 1.
      STH = 0.
      GOTO 1002

   When a large angle scatter is possible, the small angle portion
   is determined first using the Jordan-Mack small angle
   approximation equation:

   10 XMP = 1.
      BST = 1./FST
      P1 = FST*(DLOG(ARG/ETA)-1. + ETA*RARG)
      THE2= 2 * P1
      TARG = 1. -DEXP(-PI*PI/THE2)

   The multiplication term SQRT(SIN(THETA)/THETA) as suggested by
   Bethe is sampled using a rejection technique:

 1000 SARG = 1. -TARG*RAN(IRAN)
      THE = DSQRT(-THE2*DLOG(SARG))
      STH = DSIN(THE)
      REJECT = 1.
      IF (THE.GT.1.E-6) REJECT=DSQRT(STH/THE)
      IF (RAN(IRAN).GT.REJECT) GOTO 1000

      COM=DCOS(THE)

   Initialization of arrays for the large angle portion:

 1002 ROT(1,1) = COM
      ROT(2,1) = 0.
```

```
       ROT(3,1) = -STH
       ROT(1,2) = 0.
       ROT(2,2) = 1.
       ROT(3,2) = 0.
       ROT(1,3) = STH
       ROT(2,3) = 0.
       ROT(3,3) = COM
       PEXP = -XMP
       ALXMP = DLOG(XMP)
```

A random value is drawn from which the probability of each large
angle scatter will be subtracted. If this random value is less
than the the possion distributed value for one deflection, no
large angle scattering will develope:

```
       POFN = RAN(IRAN)
       XTON = 0.
       POFZ = DEXP(PEXP+XTON)
       IF(POFN.LE.POFZ) GOTO 7777
```

The random walk on the possion distribution is then carried out:

```
       POFN = POFN - POFZ
       DO 2000 N=1,500
           RF=RAN(IRAN)
           CPH = DMIN1(COSMAX,DMAX1(-1.D00,HST-1.D00/(AST+BST*RF)))
           SPH = DSQRT(1.-CPH*CPH)
           THE = PI*(2.*RAN(IRAN) -1.)
           CTH = DCOS(THE)
           STH = DSIN(THE)
           R(1,1) = CPH*CTH
           R(2,1) = CPH*STH
           R(3,1) = -SPH
           R(1,2) = -STH
           R(2,2) = CTH
           R(3,2) = 0.
           R(1,3) = SPH*CTH
           R(2,3) = SPH*STH
           R(3,3) = CPH
           DO 2050 I=1,3
           DO 2040 J=1,3
               RX(J,I) = 0.
               DO 2030 K=1,3
                   RX(J,I)=RX(J,I)+ROT(J,K)*R(K,I)
2030           CONTINUE
2040       CONTINUE
2050       CONTINUE
           DO 2070 I=1,3
           DO 2060 J=1,3
               ROT(J,I) = RX(J,I)
2060       CONTINUE
2070       CONTINUE
           COM = ROT(3,3)
```

The probability of another large angle scatter is then calculated:

47

```
                        XTON = XTON + ALXMP -ALOG(FLOAT(N))
                        POF = DEXP(PEXP+XTON)
                        POFN = POFN - POF
                        IF (POFN.LE.0.) GOTO 7777

              2000 CONTINUE
              7777 RETURN
                        END
```

C. ANGDET SUBROUTINE (MOLIERE METHOD)

The Moliere approximation was programed into CYLTRAN in a similar mannor.
The same delete and inserts for the subroutine ANGLE that were used for the Jordan-
Mack method were used for the Moliere update.

```
*INSERT ANGLE.190
      SUBROUTINE ANGDET(COM,SHD,E,RHO,Z,A)
      DOUBLE PRECISION COM,STH,CTH,SPH,CPH,ETA,FST,HST,AST,
     1 BST,XMP,P1,THE2,TARG,SARG,THE,ROT,PEXP,ALXMP,POFN
      DOUBLE PRECISION R,RX,RF,RARG,ARG,COSMAX,POF,POFZ,XTON
      DOUBLE PRECISION DSEED,IRAN,C1,C2,BK,B,REJECT
      DOUBLE PRECISION CF,C3,A1,A2,A3
      DOUBLE PRECISION ALPHA,B2,Z
      COMMON /VAXRAN/ IRAN
      DATA PI,RZERO,EMZERO,ALPHA,AVA/3.1415926536D00,0.281751
     1,0.511,137.0371,0.6025/
      RAN(DSEED)=GGUBFS(DSEED)

      Initialization of the constants:

      ET=E/EMZERO + 1.
      B21= 1./(ET*ET)
      B2= 1.-B21
      Z3= Z**.333333
      ETA = .5*(B21/B2)*(Z3/(.885*ALPHA))**2
     1 *(1.13 + 3.76*(Z/ALPHA)**2/B2)
      FST = 2.*PI*RZERO**2 *Z*(Z+1) *B21/(B2*B2)
     1 *(AVA/A)*SHD*RHO

      Evaluation of the integral values:

      HST = 1.+ETA
      AST = 1./(HST+1.0)
      RARG = 1./FST + 1./(2.+ETA)
      ARG = 1./RARG
      COSMAX = HST - ARG
      BST = 1./FST

      Evaluation of Moliere constants:

      IF (Z.EQ.13.D00) CF=-5.2D00
      IF (Z.EQ.29.D00) CF=-5.6D00
      IF (Z.EQ.79.D00) CF=-6.2D00
```

```
          IF (Z.EQ.82.D00) CF=-6.3D00
          C2=6*FST/(7*ETA)
          C1=DLOG(C2)
          A1=1.0D00
          A2=0.160D00
          A3=3.33D00
          C3=(DLOG(A2*Z3*Z3*(A1+A3*((Z/ALPHA)**2/B2)))-CF)/(Z+A1)
```

An alternate Jordan-Mack small angle approximation is done if
the value of the constant C1 is less than one. This was done
because Moliere's iterative equation diverges when C1 is less
than 1.0.

```
          IF (C1.GT.1.0D00) THEN
              BK=1.01D00
      444     B=BK
              BK=DLOG(B)+C1+C3
              IF (ABS(BK-B).GT.1.0D-4) GOTO 444
              THE2=2.0D00*FST*B
              GOTO 446
          ENDIF

      445 THE2=2*FST*(DLOG(ARG/ETA)-1.0D00+ETA*RARG)
      446 TARG = 1.0D00 -DEXP(-PI*PI/THE2)
```

   Again the multiplication factor is incorporated into the
   distribution:

```
     1000 SARG = 1.0D00 -TARG*RAN(IRAN)
          THE = DSQRT(-THE2*DLOG(SARG))
          STH = DSIN(THE)
          REJECT = 1.0D00
          IF (THE.GT.1.E-6) REJECT=DSQRT(STH/THE)
          IF (RAN(IRAN).GT.REJECT) GOTO 1000
          COM=DCOS(THE)
          RETURN
          END
```

APPENDIX D.   FORTRAN SUBROUTINE JORDAN

```
   PROGRAM JORDAN
   DOUBLE PRECISION COM
   DOUBLE PRECISION IRAN,DSEED
   COMMON /VXRAN/ IRAN
   COMMON /DANS/
  1 NDAN1,   NDAN2,   NDAN3, NDAN4, NDANM
   DIMENSION DEG(100),CEG(100),HIS(99),FLX(99)
   RANNO(DSEED)=GGUBFS(DSEED)
   IRAN=63939
   NDAN1=0
   NDAN2=0
   NDAN3=0
   NDAN4=0
   NDANM=0
   NCNT=0
   OPEN (50,FILE='JINPUT',STATUS='OLD')
   OPEN (70,FILE='XYZ9')
  1 FORMAT(/,/,/)
   WRITE (*,1)
   WRITE (*,*) '          JORDANS PROGRAM'
   WRITE (*,*)
   WRITE (*,*) '          OPTIONS:    4. MODEL4 (SMALL AND LARGE)'
   WRITE (*,*) '                      5. MODEL5 (MOLIERE)'
   WRITE (*,*) '                      6. MODEL6 (LARGE ONLY)'
   WRITE (*,*) '                      7. MODEL7 (SMALL ONLY)'
   WRITE (*,*)
   WRITE (*,*) '       ENTER:'
   READ(*,*) NOPT
   READ (50,*)
   READ (50,*)
   READ (50,*) E,SHD,RHO,Z,A
   READ (50,*)
   READ (50,*) NUMHIS,NUMBIN
   READ (50,*)
   RHOP=RHO*1000
   WRITE (70,*)
   WRITE (70,*)
   WRITE (70,*)
   WRITE (70,44) RHOP,Z,E,NUMHIS,NOPT
 44 FORMAT(F5.2,'G/CM2','   MATZ:',F5.2,'  E:',F5.2,'MEV  HIS:',I6,'M
  $ODEL:',I1)
   NZERO=0
   NTWO=2
   NFOUR=4
   NONE=1
   NTHR=3
   WRITE (70,*)
   WRITE (70,*)
   WRITE (70,*)
   WRITE (70,*) NONE,NONE,NZERO,NZERO
   WRITE (70,*) NONE,NZERO,NTWO,NZERO
```

```
      WRITE (70,*)
      WRITE (70,*)
      WRITE (70,*)
      WRITE (70,*) NTHR,NONE,NONE,NONE
      WRITE (70,'(A8)') ' JORDAN'
      NUMBIP=NUMBIN-1
      WRITE (70,*) NUMBIP
      WRITE (70,*)
      IF (NUMBIN.LE.0) GOTO 9999
      READ (50,*) (DEG(I),I=1,NUMBIN),DEG(NUMBIN+1)
      DO 1010 I=1,NUMBIN
          CEG(I)=COS(DEG(I)*3.1415926536/180.)
          HIS(I)=0.0
          FLX(I)=0.0
1010  CONTINUE
      DO 2000 N=1,NUMHIS
          IF (NOPT.EQ.4) THEN
              CALL ANGDT4(COM,SHD,E,RHO,Z,A)
          ELSE IF (NOPT.EQ.5) THEN
              CALL ANGDT5(COM,SHD,E,RHO,Z,A)
          ELSE IF (NOPT.EQ.6) THEN
              CALL ANGDT6(COM,SHD,E,RHO,Z,A)
          ELSE IF (NOPT.EQ.7) THEN
              CALL ANGDT7(COM,SHD,E,RHO,Z,A)
          ENDIF
          DO 1020 I=1,NUMBIN
              IF (COM.GE.CEG(I+1)) GOTO 1030
1020      CONTINUE
          I=NUMBIN
1030      HIS(I)=HIS(I)+1.0
          IF(HIS(I).GT.HMAX) THEN
              HMAX=HIS(I)
          ENDIF
2000  CONTINUE
      XHIS=NUMHIS
      DO 2010 I=1,NUMBIN
          IF (HIS(I).LE.0.) GOTO 2010
          ERR=100.*SQRT((XHIS-HIS(I))/((XHIS-1.)*HIS(I)))
          DEGREE=(DEG(I)+DEG(I+1))/2.0
          IF (I.EQ.1) THEN
              DEGMIN=DEGREE
          ENDIF
          NER=ERR
          NCNT=NCNT+1
          WRITE (70,*) DEGREE,HIS(I),NER
2010  CONTINUE
      WRITE (70,*) DEGMIN,DEGREE
      WRITE (70,*) NZERO,HMAX
      WRITE (70,*) '**********LOOPS INFO***********'
      WRITE (70,*) NDAN1
      WRITE (70,*) NDAN2
      WRITE (70,*) NDAN3
      WRITE (70,*) NDAN4
      WRITE (70,*) NDANM
9999  STOP
```

```
      END
C**********************************************************************************
      SUBROUTINE ANGDT4(COM,SHD,E,RHO,Z,A)
      DOUBLE PRECISION COM,STH,CTH.SPH,CPH,ETA,FST,HST,AST,
     1 BST,XMP,P1,THE2,TARG,SARG,THE,ROT,PEXP,ALXMP,POFN
      DOUBLE PRECISION R,RX,RF,RARG,ARG,COSMAX,POF,POFZ,XTON
      DOUBLE PRECISION DSEED,IRAN
      COMMON /VXRAN/ IRAN
      COMMON /DANS/
     1 NDAN1,   NDAN2,   NDAN3, NDAN4, NDANM
      DIMENSION ROT(3,3),R(3,3),RX(3,3)
      RANNO(DSEED)=GGUBFS(DSEED)
      DATA PI,RZERO,EMZERO,ALPHA,AVA/3.1415926536D00,0.281751
     1,0.511,137.0371,0.6025/
      ET=E/EMZERO + 1.
      B21= 1./(ET*ET)
      B2= 1.-B21
      Z3= Z**.333333
      ETA = .5*(B21/B2)*(Z3/(.885*ALPHA))**2
     1 *(1.13 + 3.76*(Z/ALPHA)**2/B2)
      FST = 2.*PI*RZERO**2 *Z*(Z+1) *B21/(B2*B2)
     1 *(AVA/A)*SHD*RHO
      HST = 1.+ETA
      AST = 1./(HST+1.0)
      RARG = 1./FST + 1./(2.+ETA)
      ARG = 1./RARG
      COSMAX = HST - ARG
      NDAN1=NDAN1+1
  144 IF (COSMAX.LT.1.) GOTO 10
      NDAN2=NDAN2+1
      COSMAX = 1.0
      BST = 1./ETA -AST
      XMP = FST*BST
      COM = 1.
      STH = 0.
      GOTO 1002
   10 XMP = 1.
      NDAN3=NDAN3+1 ·
      BST = 1./FST
      P1 = FST*(DLOG(ARG/ETA)-1. + ETA*RARG)
      THE2 = 2.*P1
      TARG = 1. -DEXP(-PI*PI/THE2)
 1000 SARG = 1. -TARG*RANNO(IRAN)
      THE = DSQRT(-THE2*DLOG(SARG))
      STH = DSIN(THE)
      REJECT = 1.
      IF (THE.GT.1.E-6) REJECT=DSQRT(STH/THE)
      IF (RANNO(IRAN).GT.REJECT) GOTO 1000
      COM=DCOS(THE)
 1002 ROT(1,1) = COM
      ROT(2,1) = 0.
      ROT(3,1) = -STH
      ROT(1,2) = 0.
      ROT(2,2) = 1.
      ROT(3,2) = 0.
      ROT(1,3) = STH
```

```fortran
      ROT(2,3) = 0.
      ROT(3,3) = COM
      PEXP = -XMP
      ALXMP = DLOG(XMP)
      POFN = RANNO(IRAN)
      XTON = 0.
      POFZ = DEXP(PEXP+XTON)
      IF(POFN.LE.POFZ) GOTO 7777
      NDAN4=NDAN4+1
      POFN = POFN - POFZ
      DO 2000 N=1,500
           IF (N.GT.NDANM) THEN
                NDANM=N
           ENDIF
           RF=RANNO(IRAN)
      CPH = DMIN1(COSMAX,DMAX1(-1.D00,HST-1.D00/(AST+BST*RF)))
           SPH = DSQRT(1.-CPH*CPH)
           THE = PI*(2.*RANNO(IRAN) -1.)
           CTH = DCOS(THE)
           STH = DSIN(THE)
           R(1,1) = CPH*CTH
           R(2,1) = CPH*STH
           R(3,1) = -SPH
           R(1,2) = -STH
           R(2,2) = CTH
           R(3,2) = 0.
           R(1,3) = SPH*CTH
           R(2,3) = SPH*STH
           R(3,3) = CPH
           DO 2050 I=1,3
           DO 2040 J=1,3
               RX(J,I) = 0.
               DO 2030 K=1,3
                   RX(J,I)=RX(J,I)+ROT(J,K)*R(K,I)
2030           CONTINUE
2040       CONTINUE
2050       CONTINUE
           DO 2070 I=1,3
           DO 2060 J=1,3
               ROT(J,I) = RX(J,I)
2060       CONTINUE
2070       CONTINUE
           COM = ROT(3,3)
           XTON = XTON + ALXMP -ALOG(FLOAT(N))
           POF = DEXP(PEXP+XTON)
           POFN = POFN - POF .
           IF (POFN.LE.0.) GOTO 7777
2000  CONTINUE
7777  RETURN
      END
C*************************************************************************
      SUBROUTINE ANGDT5(COM,SHD,E,RHO,Z,A)
      DOUBLE PRECISION COM,STH,CTH,SPH,CPH,ETA,FST,HST,AST,
     1 BST,XMP,P1,THE2,TARG,SARG,THE,ROT,PEXP,ALXMP,POFN
      DOUBLE PRECISION R,RX,RF,RARG,ARG,COSMAX,POF,POFZ,XTON
      DOUBLE PRECISION DSEED,IRAN,C1,C2,BK,B,REJECT
```

```fortran
      DOUBLE PRECISION CF,C3,A1,A2,A3
      DOUBLE PRECISION ALPHA,B2,Z
      COMMON /VXRAN/ IRAN
      COMMON /DANS/
     1 NDAN1,   NDAN2,  NDAN3, NDAN4, NDANM
      DATA PI,RZERO,EMZERO,ALPHA,AVA/3.1415926536D00,0.281751
     1,0.511,137.0371,0.6025/
      RANNO(DSEED)=GGUBFS(DSEED)
      ET=E/EMZERO + 1.
      B21= 1./(ET*ET)
      B2= 1.-B21
      Z3= Z**.333333
      ETA = .5*(B21/B2)*(Z3/(.885*ALPHA))**2
     1 *(1.13 + 3.76*(Z/ALPHA)**2/B2)
      FST = 2.*PI*RZERO**2 *Z*(Z+1) *B21/(B2*B2)
     1 *(AVA/A)*SHD*RHO
      HST = 1.+ETA
      AST = 1./(HST+1.0)
      RARG = 1./FST + 1./(2.+ETA)
      ARG = 1./RARG
      COSMAX = HST - ARG
      NDAN1=NDAN1+1
      BST = 1./FST
      CF=-6.2D00
      C2=6*FST/(7*ETA)
      C1=DLOG(C2)
      A1=1.0D00
      A2=0.160D00
      A3=3.33D00
      C3=(DLOG(A2*Z3*Z3*(A1+A3*((Z/ALPHA)**2/B2)))-CF)/(Z+A1)
      IF (C1.GT.1.0D00) THEN
          BK=1.01D00
  444     B=BK
          BK=DLOG(B)+C1+C3
          IF (ABS(BK-B).GT.1.0D-4) GOTO 444
          THE2=2.0D00*FST*B
          GOTO 446
      ENDIF
  445 THE2=2*FST*(DLOG(ARG/ETA)-1.0D00+ETA*RARG)
      NDAN2=NDAN2+1
  446 TARG = 1.0D00 -DEXP(-PI*PI/THE2)
 1000 SARG = 1.0D00 -TARG*RANNO(IRAN)
      THE = DSQRT(-THE2*DLOG(SARG))
      STH = DSIN(THE)
      REJECT = 1.0D00
      IF (THE.GT.1.E-6) REJECT=DSQRT(STH/THE)
      IF (RANNO(IRAN).GT.REJECT) GOTO 1000
      COM=DCOS(THE)
      RETURN
      END
C************************************************************************
      SUBROUTINE ANGDT6(COM,SHD,E,RHO,Z,A)
      DOUBLE PRECISION COM,STH,CTH,SPH,CPH,ETA,FST,HST,AST,
     1 BST,XMP,P1,THE2,TARG,SARG,THE,ROT,PEXP,ALXMP,POFN
      DOUBLE PRECISION R,RX,RF,RARG,ARG,COSMAX,POF,POFZ,XTON
      DOUBLE PRECISION IRAN,DSEED
```

54

```fortran
      COMMON /VXRAN/ IRAN
      COMMON /DANS/
     1 NDAN1,   NDAN2,  NDAN3, NDAN4, NDANM
      DIMENSION ROT(3,3),R(3,3),RX(3,3)
      DATA PI,RZERO,EMZERO,ALPHA,AVA/3.1415926536D00,0.281751
     1,0.511,137.0371,0.6025/
      RANNO(DSEED)=GGUBFS(DSEED)
      ET=E/EMZERO + 1.
      B21= 1./(ET*ET)
      B2= 1.-B21
      Z3= Z**.333333
      ETA = .5*(B21/B2)*(Z3/(.885*ALPHA))**2
     1 *(1.13 + 3.76*(Z/ALPHA)**2/B2)
      FST = 2.*PI*RZERO**2 *Z*(Z+1) *B21/(B2*B2)
     1 *(AVA/A)*SHD*RHO
      HST = 1.+ETA
      AST = 1./(HST+1.0)
      RARG = 1./FST + 1./(2.+ETA)
      ARG = 1./RARG
      COSMAX = HST - ARG
      NDAN1=NDAN1+1
  144 IF (COSMAX.LT.1.) GOTO 10
      NDAN2=NDAN2+1
      COM = 1.0
      GOTO 7777
   10 XMP = 1.
      NDAN3=NDAN3+1
      BST = 1./FST
      COM=1.0
      STH=0.0
 1002 ROT(1,1) = COM
      ROT(2,1) = 0.
      ROT(3,1) = -STH
      ROT(1,2) = 0.
      ROT(2,2) = 1.
      ROT(3,2) = 0.
      ROT(1,3) = STH
      ROT(2,3) = 0.
      ROT(3,3) = COM
      PEXP = -XMP
      ALXMP = DLOG(XMP)
      POFN = RANNO(IRAN)
      XTON = 0.
      POFZ = DEXP(PEXP+XTON)
      IF(POFN.LE.POFZ) GOTO 7777
      NDAN4=NDAN4+1
      POFN = POFN - POFZ
      NDANM=0
      DO 2000 N=1,500
          RF=RANNO(IRAN)
      CPH = DMIN1(COSMAX,DMAX1(-1.D00,HST-1.D00/(AST+BST*RF)))
          SPH = DSQRT(1.-CPH*CPH)
          THE = PI*(2.*RANNO(IRAN) -1.)
          CTH = DCOS(THE)
          STH = DSIN(THE)
          R(1,1) = CPH*CTH
```

55

```fortran
              R(2,1) = CPH*STH
              R(3,1) = -SPH
              R(1,2) = -STH
              R(2,2) = CTH
              R(3,2) = 0.
              R(1,3) = SPH*CTH
              R(2,3) = SPH*STH
              R(3,3) = CPH
              DO 2050 I=1,3
              DO 2040 J=1,3
                   RX(J,I) = 0.
                   DO 2030 K=1,3
                        RX(J,I)=RX(J,I)+ROT(J,K)*R(K,I)
 2030              CONTINUE
 2040         CONTINUE
 2050         CONTINUE
              DO 2070 I=1,3
              DO 2060 J=1,3
                   ROT(J,I) = RX(J,I)
 2060         CONTINUE
 2070         CONTINUE
              COM = ROT(3,3)
              XTON = XTON + ALXMP -ALOG(FLOAT(N))
              POF = DEXP(PEXP+XTON)
              POFN = POFN - POF
              IF (POFN.LE.0.) GOTO 7777
 2000 CONTINUE
 7777 RETURN
      END
C*****************************************************************************
      SUBROUTINE ANGDT7(COM,SHD,E,RHO,Z,A)
      DOUBLE PRECISION COM,STH,CTH,SPH,CPH,ETA,FST,HST,AST,
     1 BST,XMP,P1,THE2,TARG,SARG,THE,ROT,PEXP,ALXMP,POFN
      DOUBLE PRECISION R,RX,RF,RARG,ARG,COSMAX,POF,POFZ,XTON
      DOUBLE PRECISION IRAN,DSEED
      COMMON /VXRAN/ IRAN
      COMMON /DANS/
     1 NDAN1,   NDAN2,   NDAN3, NDAN4, NDANM
      DIMENSION ROT(3,3),R(3,3),RX(3,3)
      DATA PI,RZERO,EMZERO,ALPHA,AVA/3.1415926536D00,0.281751
     1,0.511,137.0371,0.6025/
      RANNO(DSEED)=GGUBFS(DSEED)
      ET=E/EMZERO + 1.
      B21= 1./(ET*ET)
      B2= 1.-B21
      Z3= Z**.333333
      ETA = .5*(B21/B2)*(Z3/(.885*ALPHA))**2
     1 *(1.13 + 3.76*(Z/ALPHA)**2/B2)
      FST = 2.*PI*RZERO**2 *Z*(Z+1) *B21/(B2*B2)
     1 *(AVA/A)*SHD*RHO
      HST = 1.+ETA
      AST = 1./(HST+1.0)
      RARG = 1./FST + 1./(2.+ETA)
      ARG = 1./RARG
      COSMAX = HST - ARG
      NDAN1=NDAN1+1
```

56

```fortran
  144 IF (COSMAX.LT.1.) GOTO 10
      NDAN2=NDAN2+1
      COSMAX = 1.0
      BST = 1./ETA -AST
      XMP = FST*BST
      COM = 1.
      STH = 0.
      GOTO 7777
   10 XMP = 1.
      NDAN3=NDAN3+1
      BST = 1./FST
      P1 = FST*(DLOG(ARG/ETA)-1. + ETA*RARG)
      THE2 = 2.*P1
      TARG = 1. -DEXP(-PI*PI/THE2)
 1000 SARG = 1. -TARG*RANNO(IRAN)
      THE = DSQRT(-THE2*DLOG(SARG))
      STH = DSIN(THE)
      REJECT = 1.
      IF (THE.GT.1.E-6) REJECT=DSQRT(STH/THE)
      IF (RANNO(IRAN).GT.REJECT) GOTO 1000
      COM=DCOS(THE)
 7777 RETURN
      END
```

57

APPENDIX E.   LARGE AND SMALL ANGLE SCATTERING
DISTRIBUTIONS

Since the Jordan-Mack correction scheme decouples the multiple scattering into large and small angle scattering, it seemed natural to plot the contribution of each separately. The FORTRAN program JORDAN was used to calculate the small and large angle scattering distributions. JORDAN is only a number tally calculation and involves only the columb scattering. Pair production, absorption, secondary production, and other particle interactions are not calculated. For very thin foils these effects are minor. The input parameters to JORDAN were for the case of the Hanson gold foil, (18.67 mg/cm²). The energy of the incident electrons was increased from 0.01 Mev to 10.0 Mev. The number of histories was 100,000 for all JORDAN runs. Figures 18 thru 24 show the small angle distributions for this case. Figures 25 thru 34 show the large angle distributions. Note the large discontinuity in the small angle distributions are at 105 degrees. When the energy is greater than 0.5 MeV this discontinuity becomes very minor.
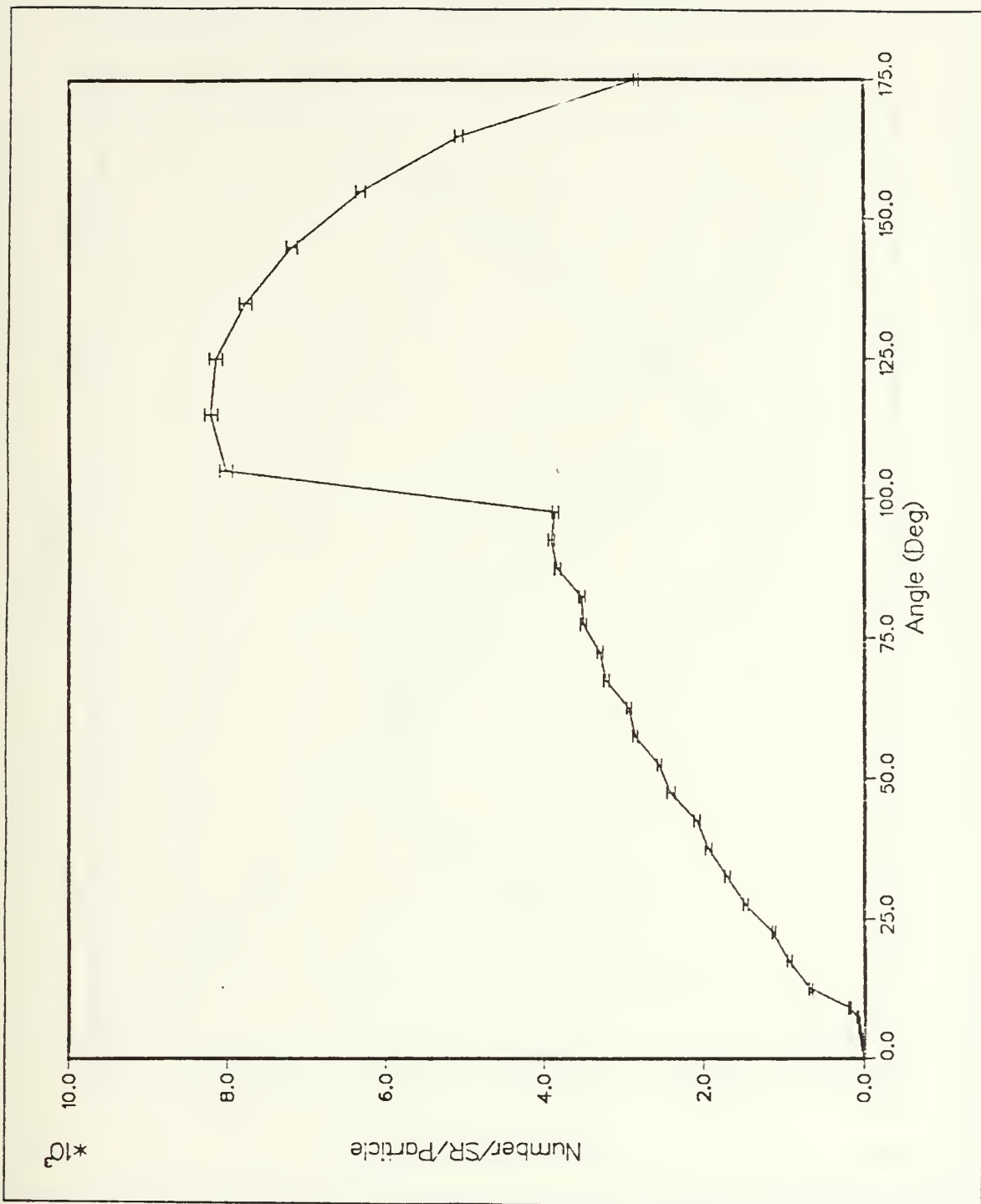
Figure 18.   Small Angle Spectrum for 0.01 MeV: The input parameters were for a 18.66 mg cm² gold foil with 0.01 MeV incident electrons.
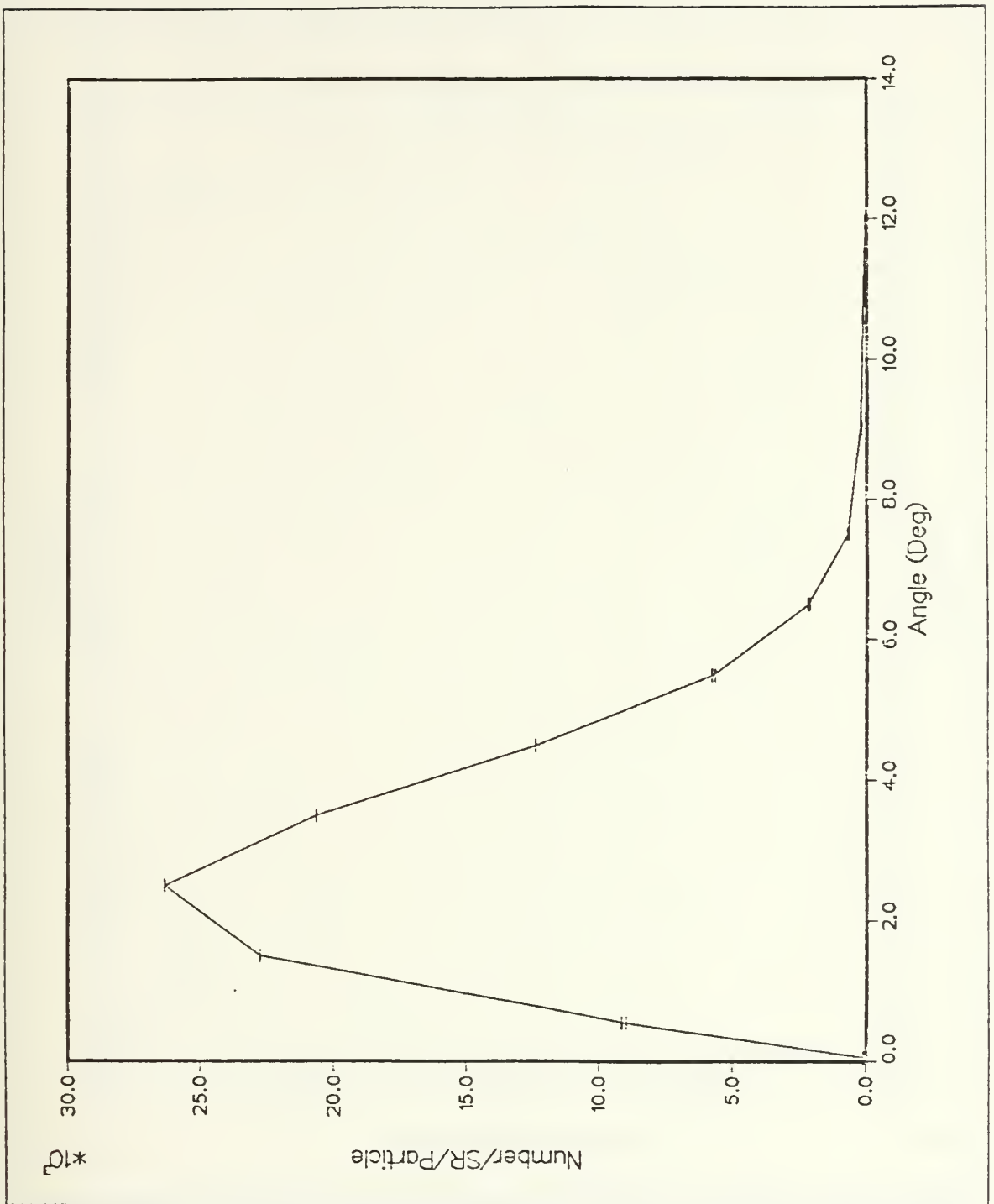
59
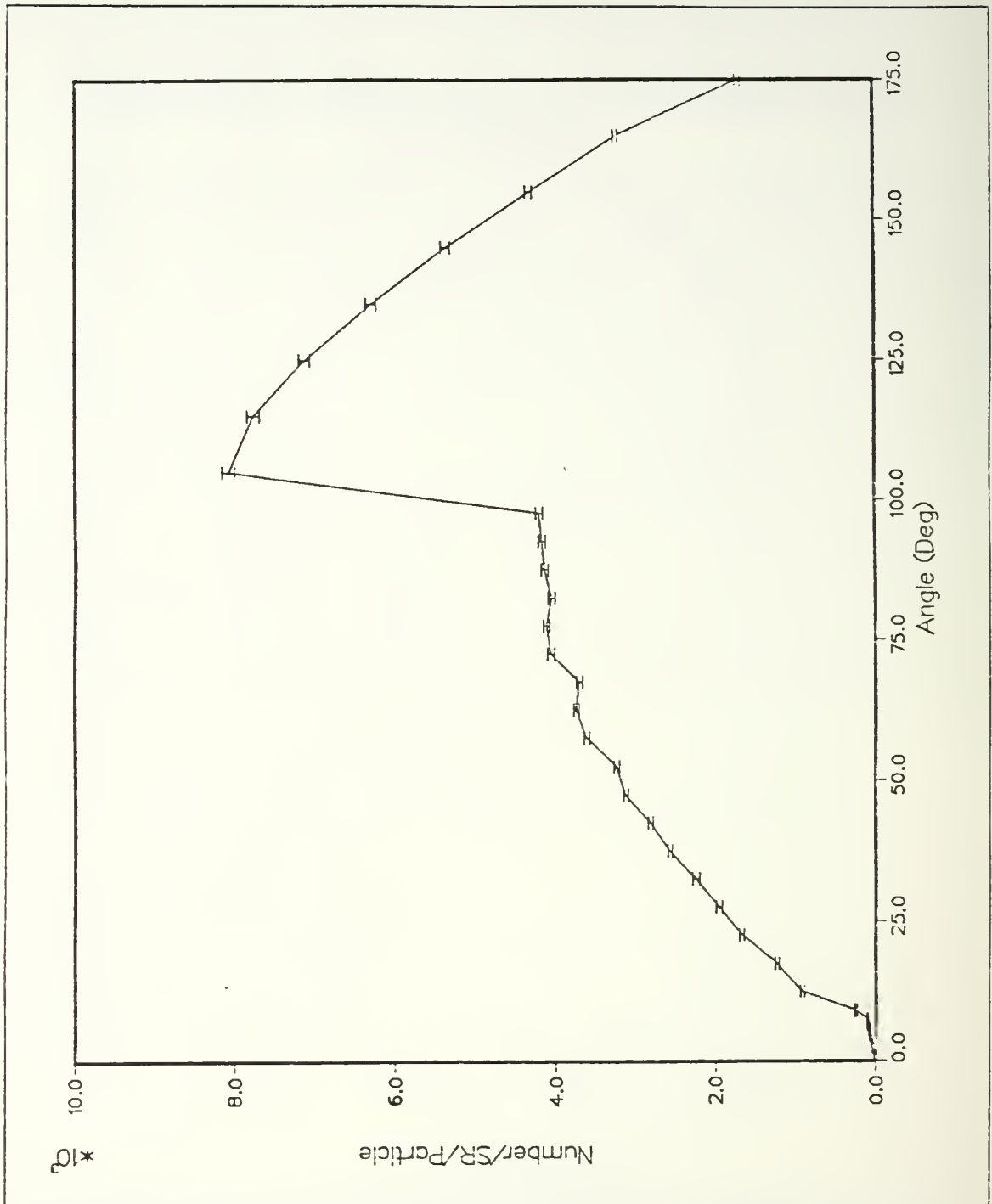
Figure 19. Small Angle Spectrum for 0.10 MeV: The input parameters were the same as Figure 18 on page 59 except the incident electron energy was 0.10 MeV.
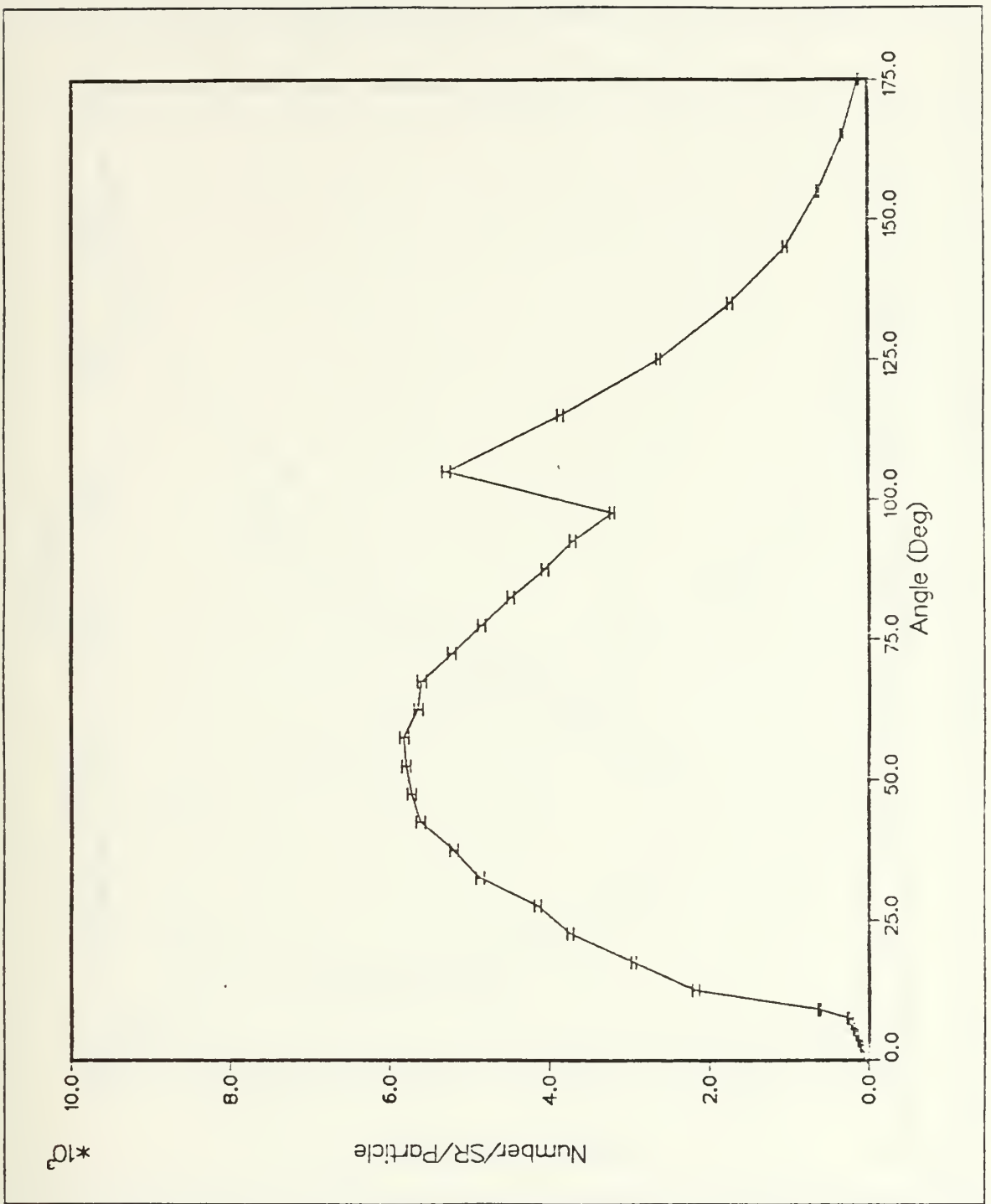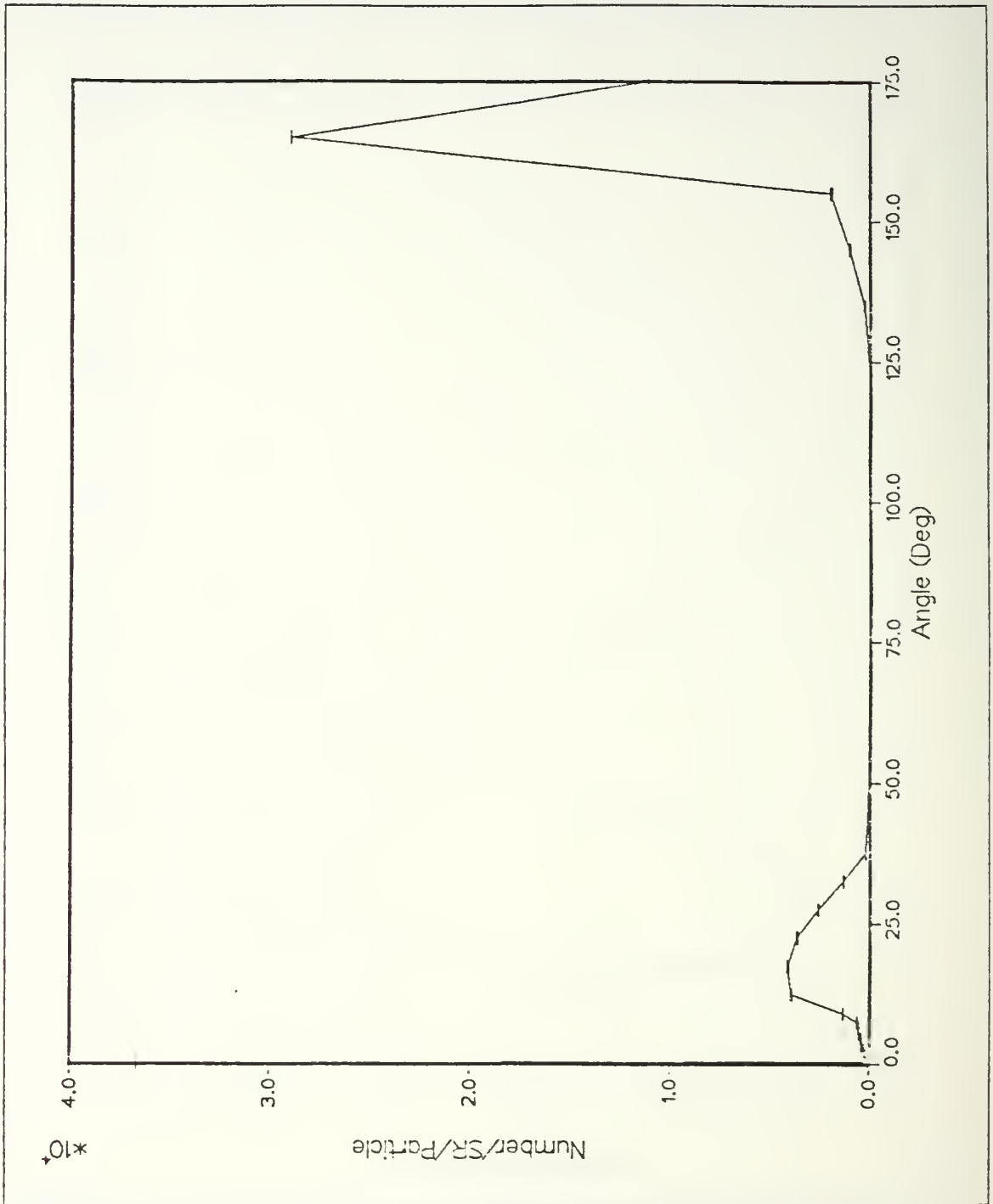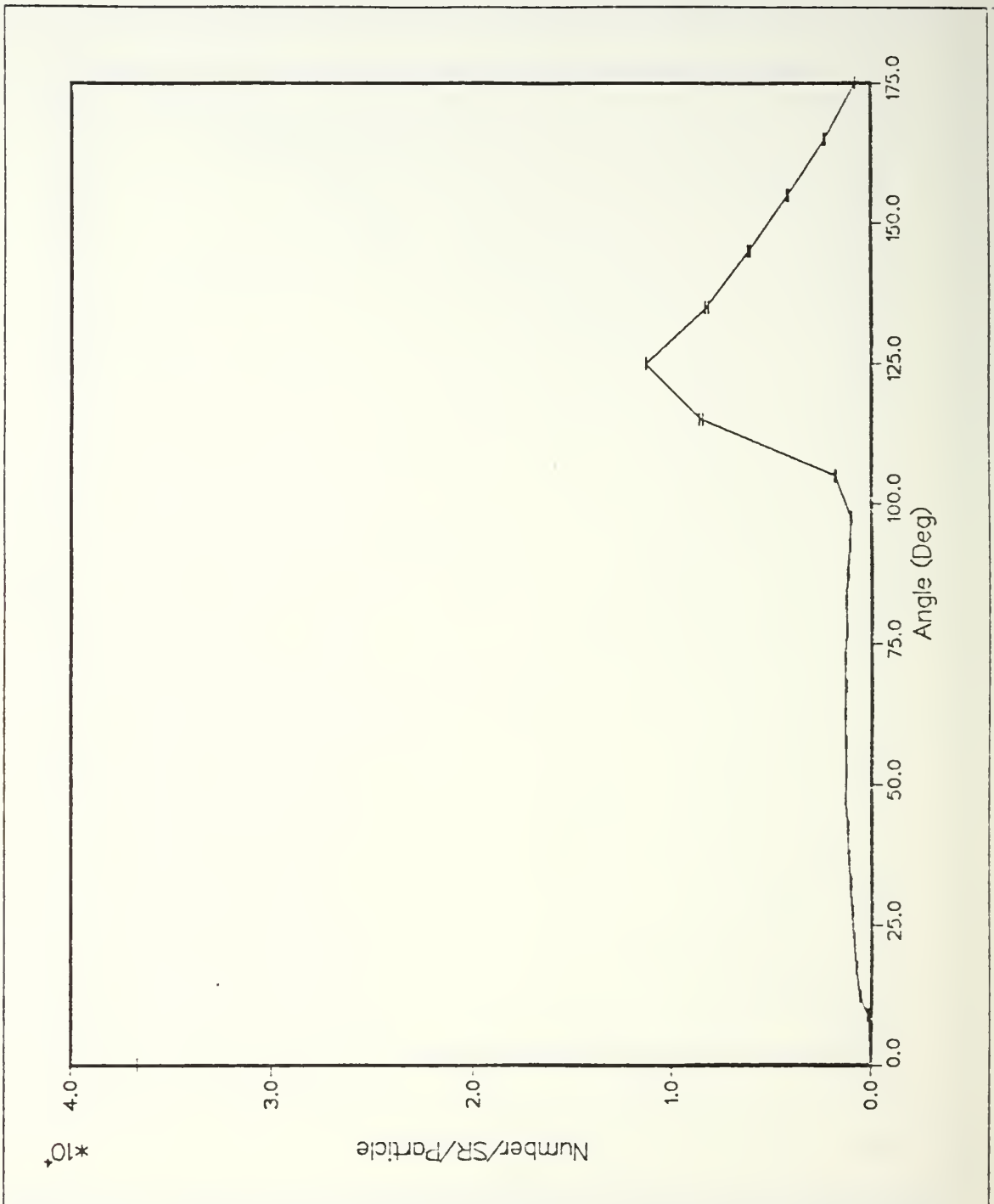
Figure 20.   Small Angle Spectrum for 0.25 MeV: The input parameters were the same as Figure 18 on page 59 except the incident electron energy was 0.25 MeV.
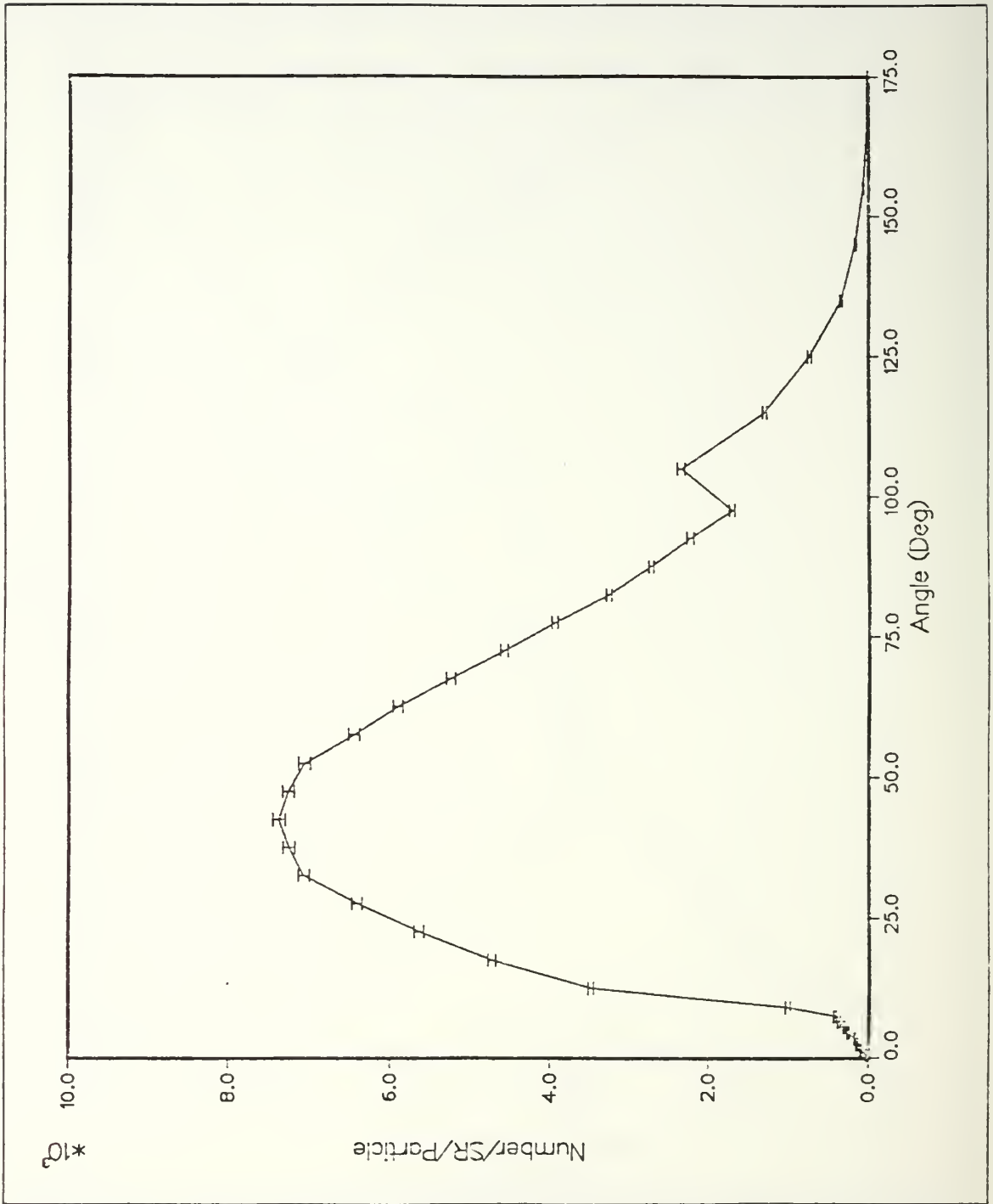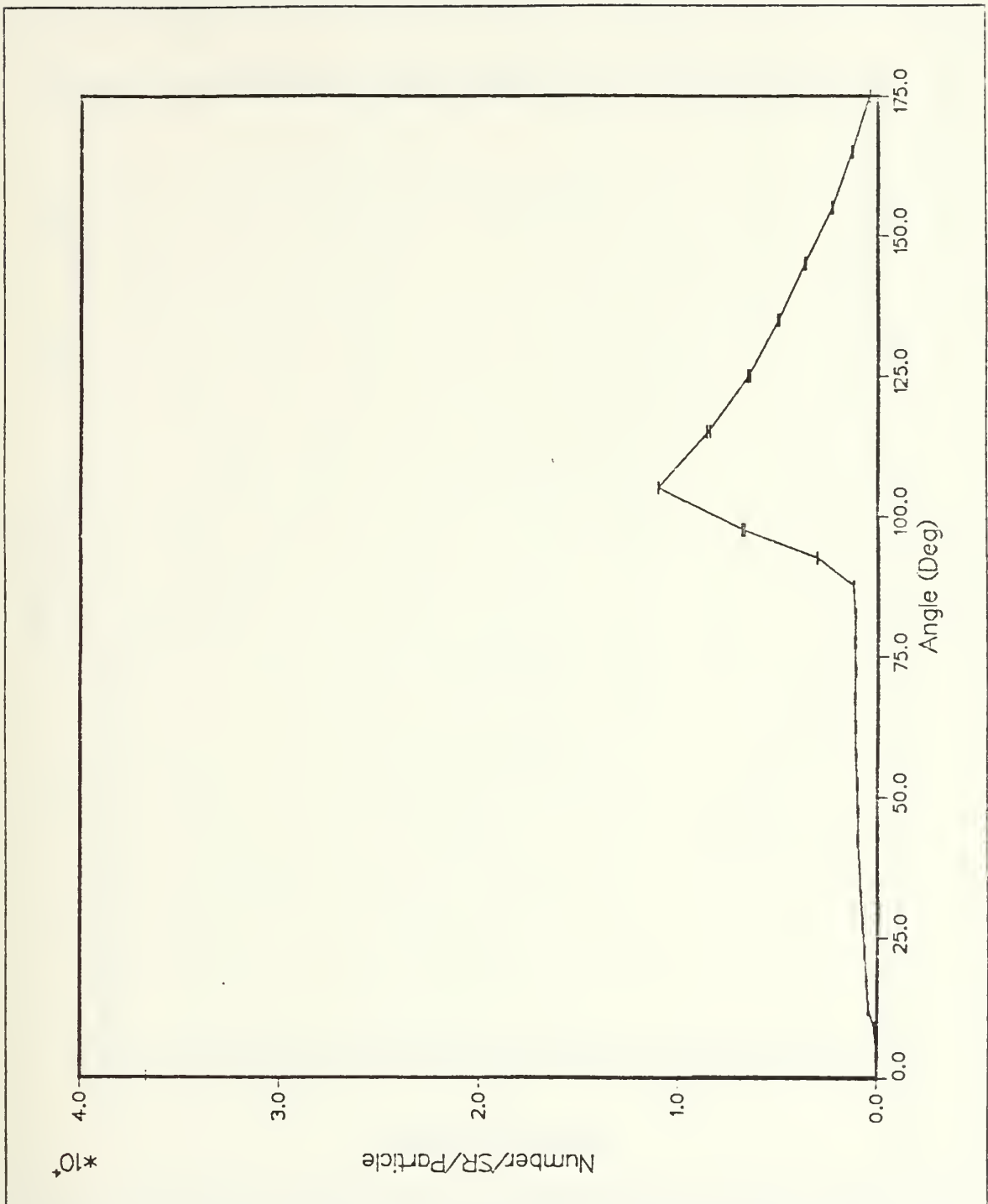
Figure 21.   Small Angle Spectrum for 0.35 MeV: The input parameters were the same as Figure 18 on page 59 except the incident electron energy was 0.35 MeV.
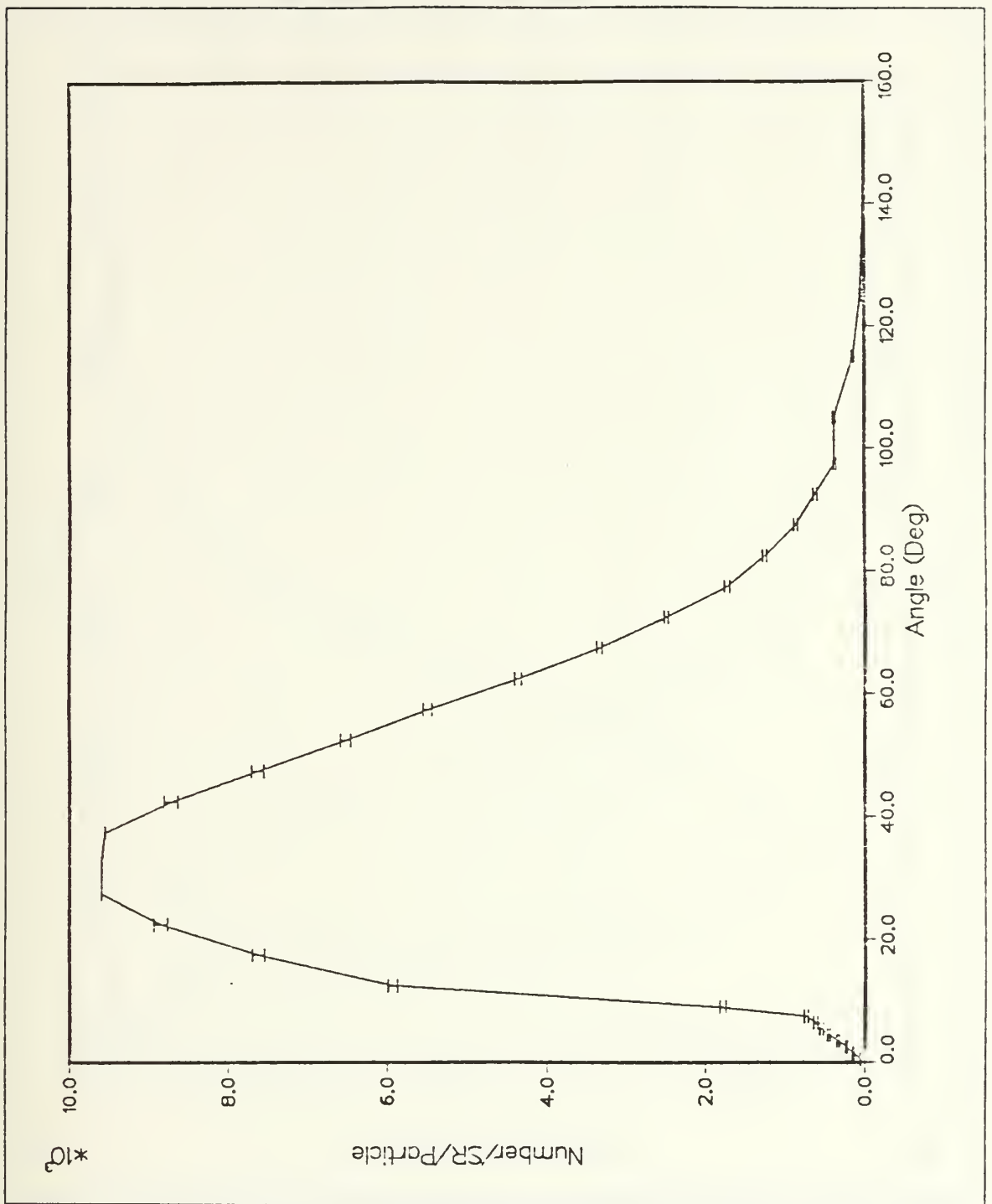
Figure 22.   Small Angle Spectrum for 0.50 MeV: The input parameters were the same as Figure 18 on page 59 except the incident electron energy was 0.50 MeV.
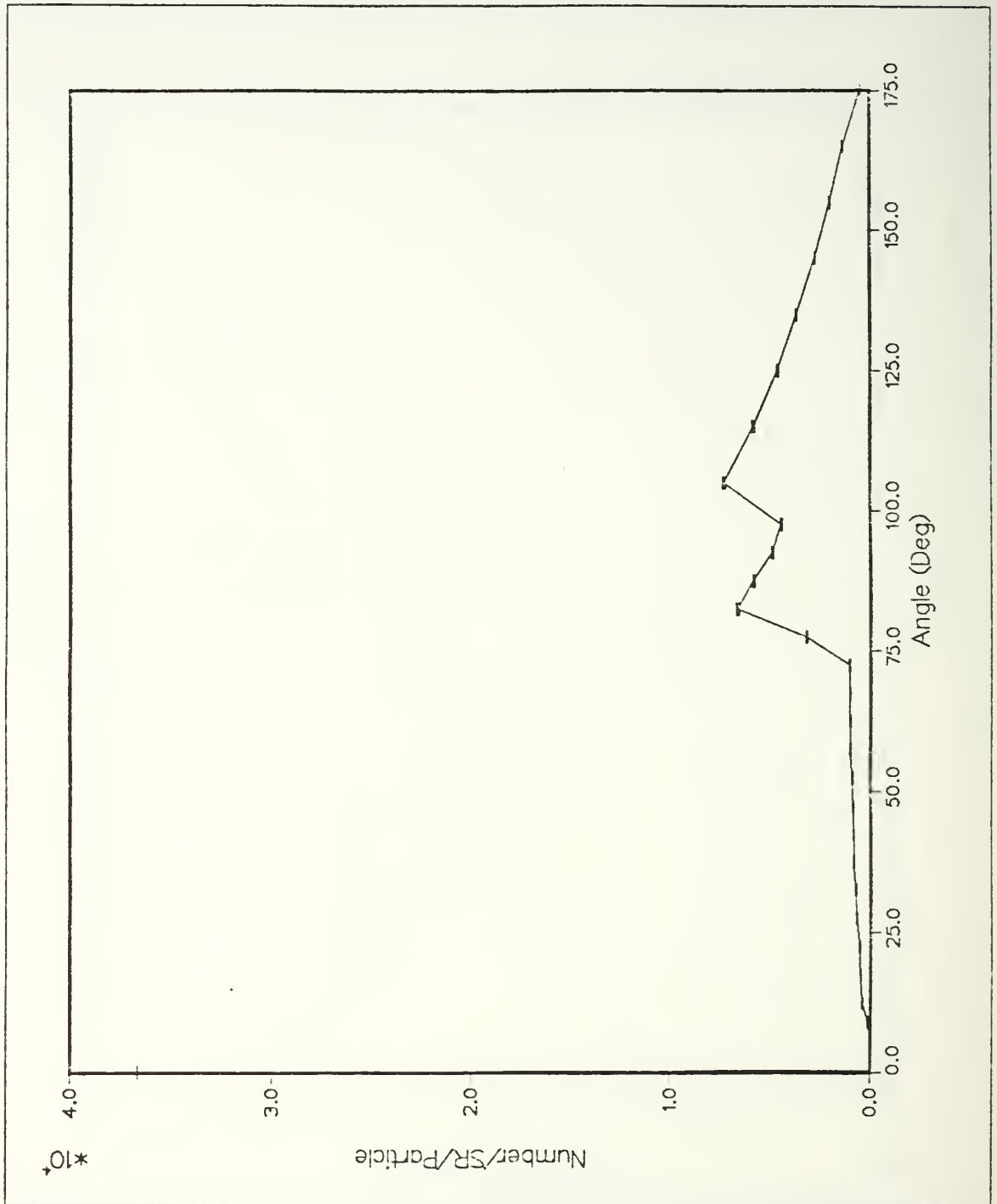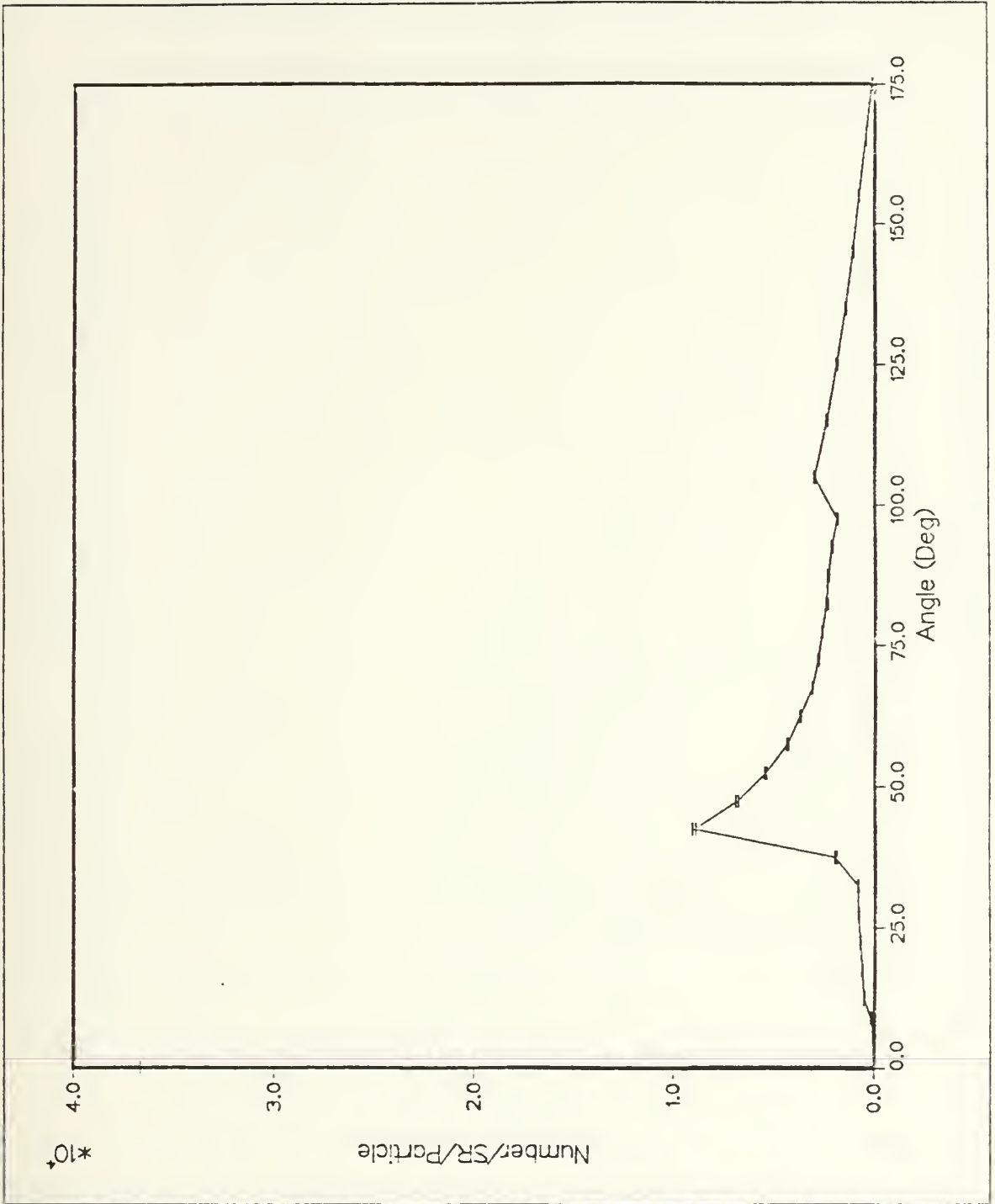
63
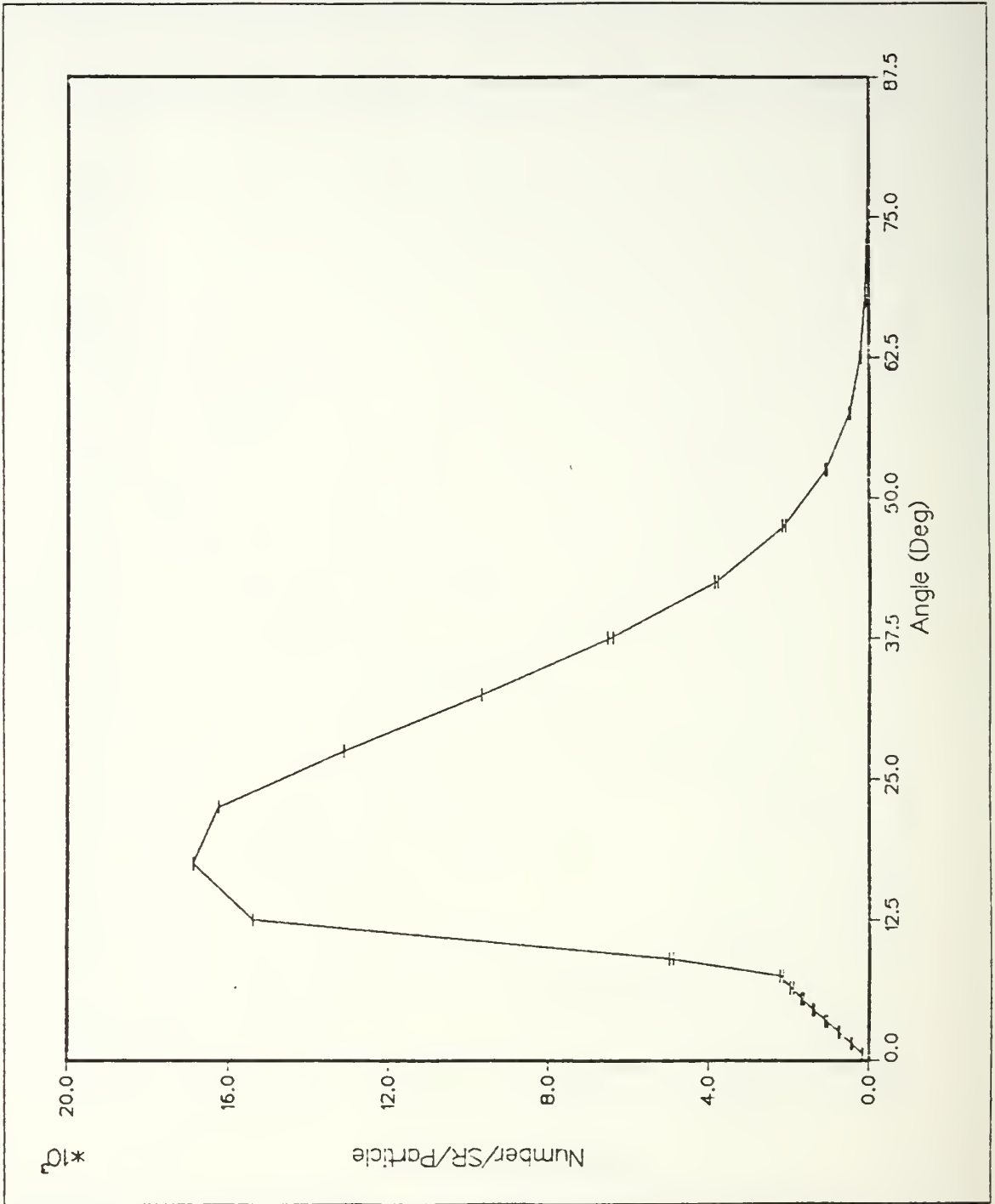
Figure 23. Small Angle Spectrum for 1.00 MeV: The input parameters were the same as Figure 18 on page 59 except the incident electron energy was 1.00 MeV.

Figure 24. Small Angle Spectrum for 10.0 MeV: The input parameters were the same as Figure 18 on page 59 except the incident electron energy was 10.0 MeV.

65

Figure 25.   Large Angle Spectrum for 0.01 MeV: The input parameters were for
a 18.66 mg cm² gold foil with 0.01 MeV incident electrons.

Figure 26.   Large Angle Spectrum for 0.02 MeV: The input parameters were the same as Figure 25 on page 66 except the incident electron energy was 0.02 MeV.
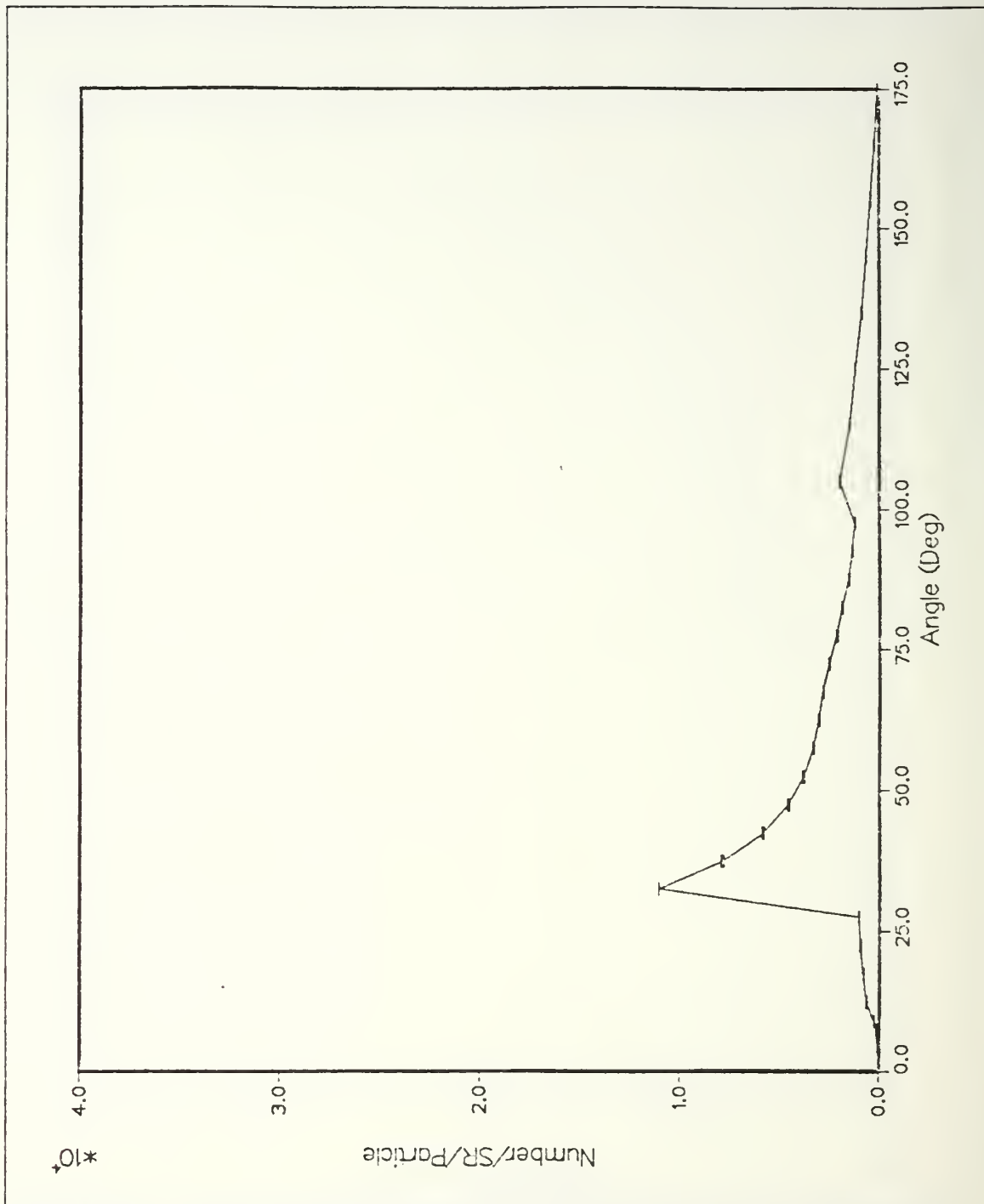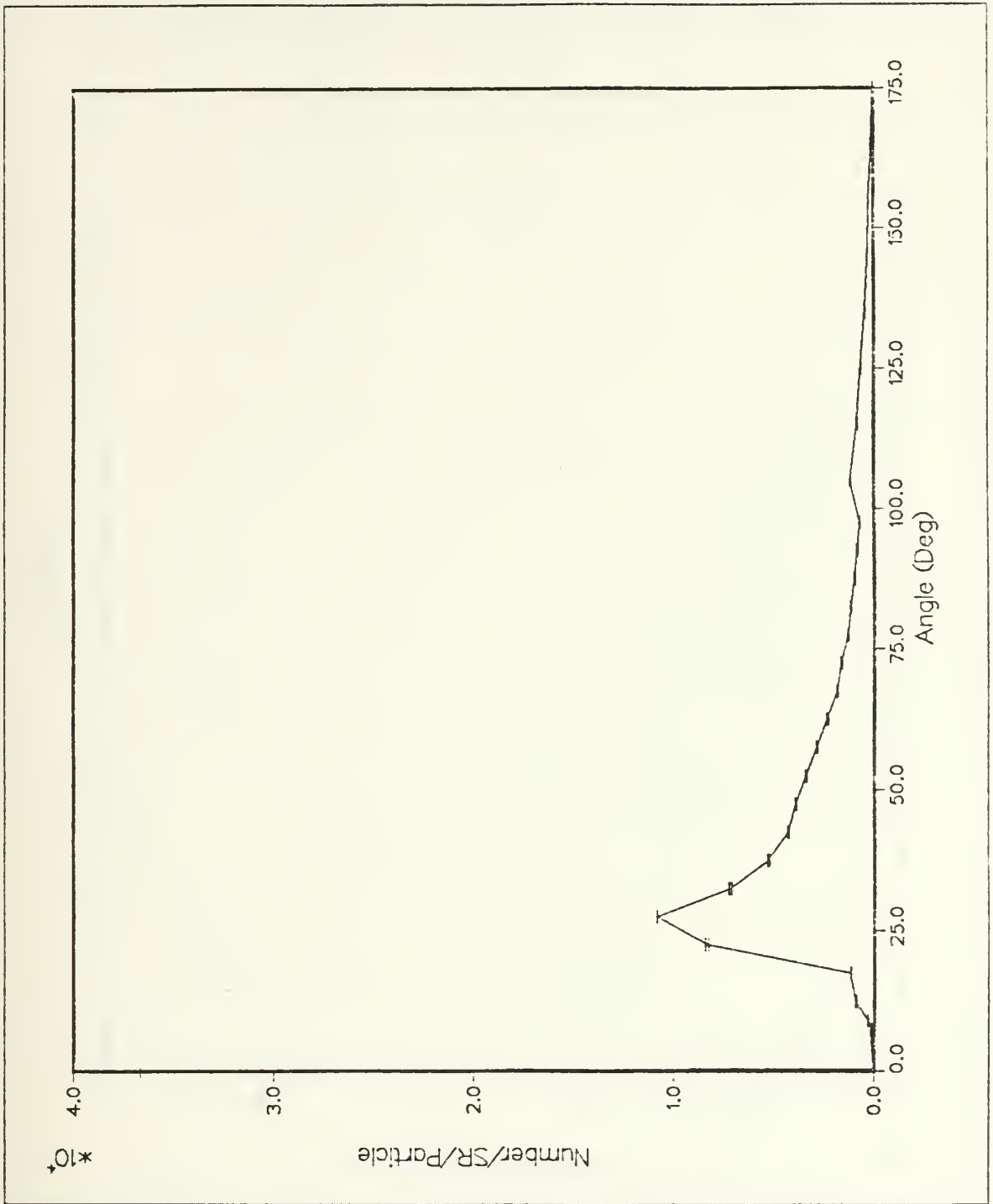
67

Figure 27. Large Angle Spectrum for 0.05 MeV: The input parameters were the same as Figure 25 on page 66 except the incident electron energy was 0.05 MeV.

Figure 28. Large Angle Spectrum for 0.07 MeV: The input parameters were the same as Figure 25 on page 66 except the incident electron energy was 0.07 MeV.

Figure 29. Large Angle Spectrum for 0.10 MeV: The input parameters were the same as Figure 25 on page 66 except the incident electron energy was 0.10 MeV.
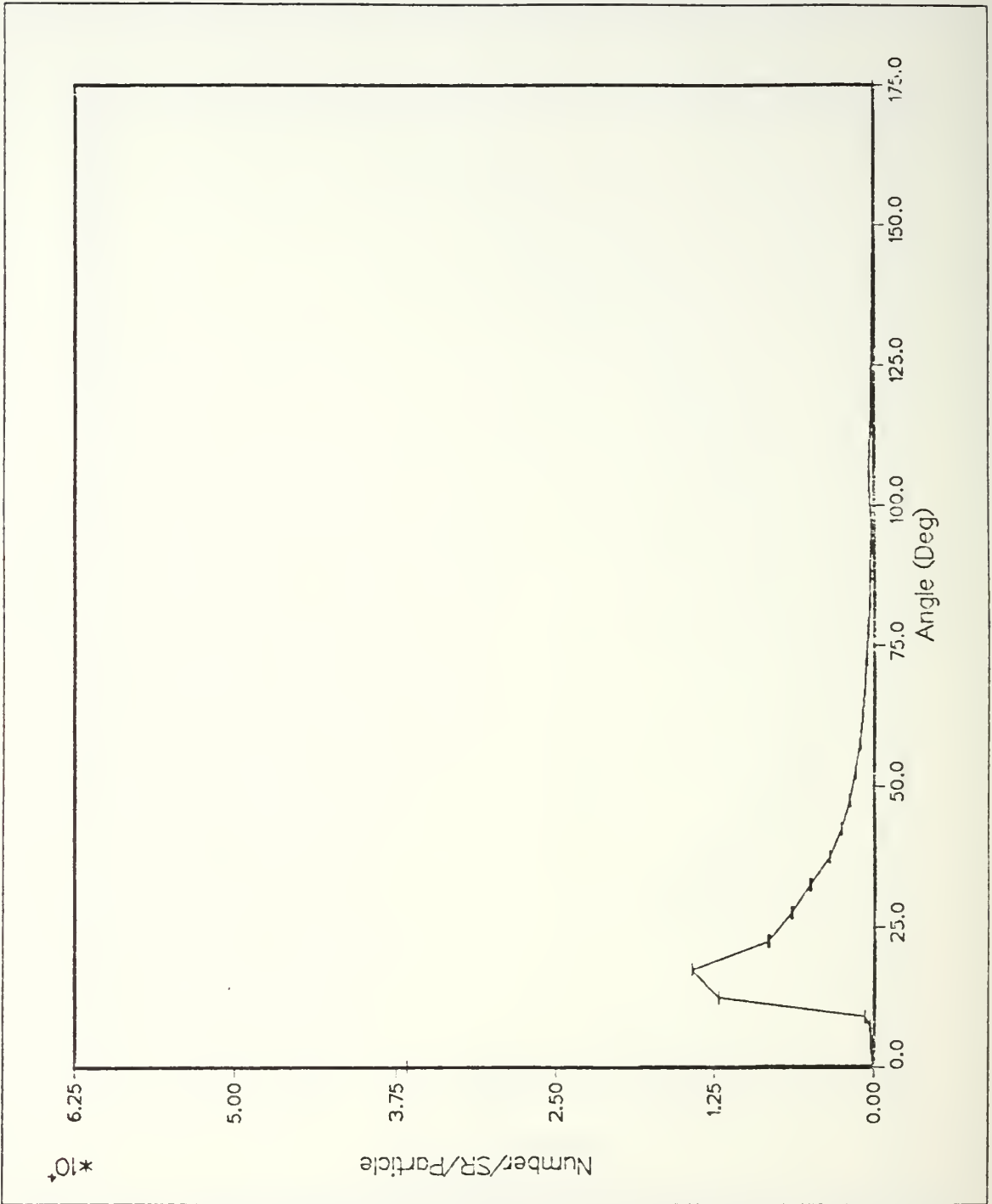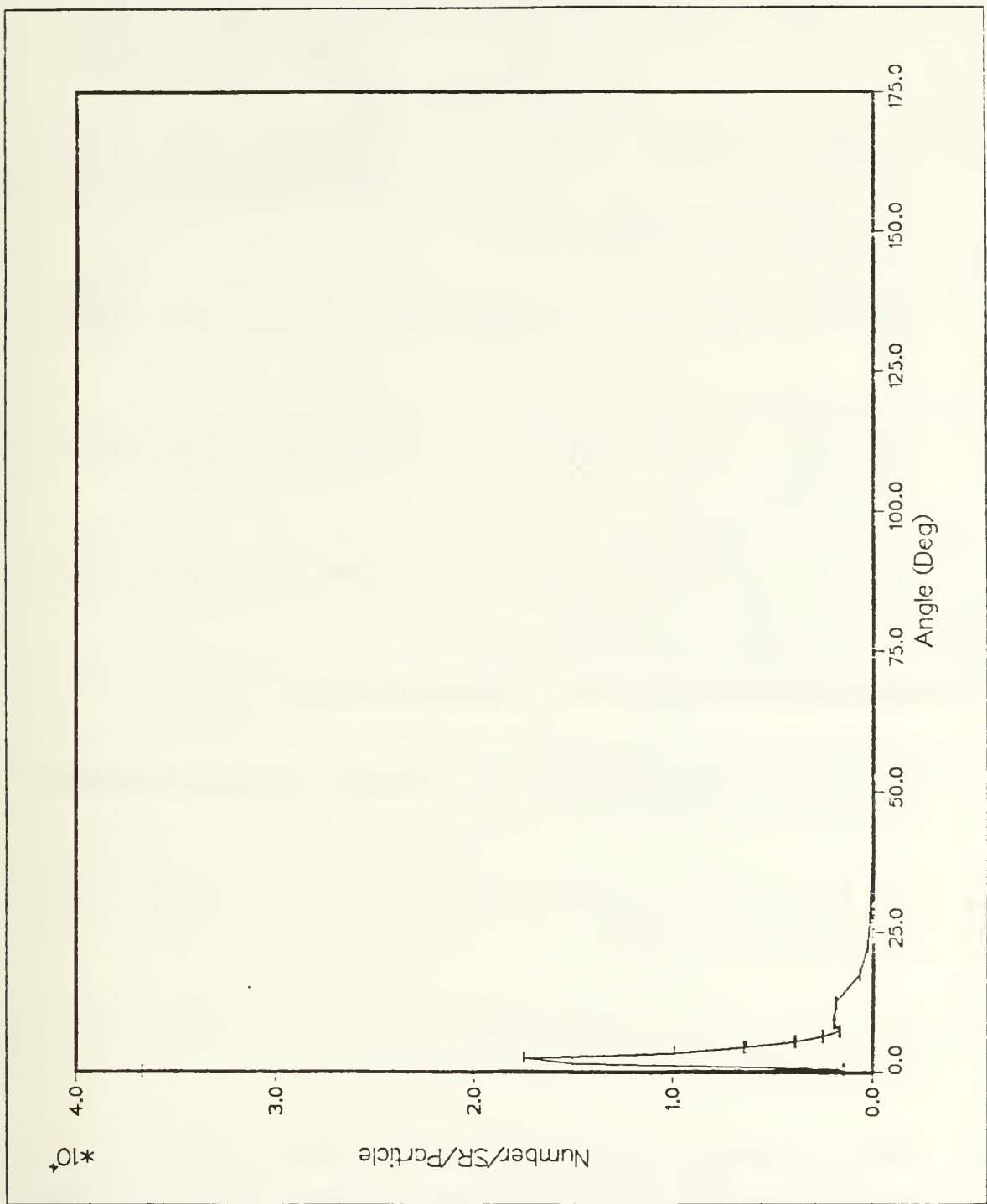
Figure 30.   Large Angle Spectrum for 0.25 MeV: The input parameters were the
same as Figure 25 on page 66 except the incident electron energy was
0.25 MeV.

Figure 31.   Large Angle Spectrum for 0.35 MeV: The input parameters were the
            same as Figure 25 on page 66 except the incident electron energy was
            0.35 MeV.

Figure 32.   Large Angle Spectrum for 0.50 MeV: The input parameters were the same as Figure 25 on page 66 except the incident electron energy was 0.50 MeV.

Figure 33.   Large Angle Spectrum for 1.00 MeV: The input parameters were the same as Figure 25 on page 66 except the incident electron energy was 1.00 MeV.

Figure 34. Large Angle Spectrum for 10.0 MeV: The input parameters were the same as Figure 25 on page 66 except the incident electron energy was 10.0 MeV.

75

LIST OF REFERENCES

1. Halbleib, J.A., Mehlhorn, T.A., *ITS: The Integrated Tiger Series of Coupled Electron Photon Monte Carlo Transport Code*, Sandia National Laboratories, Report SAND84-0573, November, 1984.

2. Berger, M.J., "Methods in Computational Physics", *Statistical Physics*, Volume 1, 1963.

3. Williams, E.J., "Concerning the Scattering of Fast Electrons and of Cosmic-Ray Particles", *Proc. Roy. Soc.*, Volume 169, p. 531, October 25, 1938.

4. Goudsmit, S., and Saunderson, J.L., "Multiple Scattering of Electrons", *Physical Review*, Volume 57, p. 24, November 8, 1939.

5. Moliere, G., "Multiple Scattering", *Naturforsch*, Volume 3a, p. 78, 1948.

6. Synder, H.S., and Scott, W.T., "Multiple Scattering of Fast Charged Particles", *Physical Review*, Volume 76, p. 220, February 11, 1949.

7. Lewis, H.W., "Multiple Scattering in an Infinite Medium", *Physical Review*, Volume 78, p. 526, January 24, 1950.

8. Bothe, Von W., "Die Streuabsoption der Elektronenstrahlen", *Z. Phys.*, Volume 54 p. 161, February 15, 1929.

9. Nigam, B.P., Sundaresan, M.K., and Ta-You Wu, "Theory of Multiple Scattering: Second Born Approximation and Corrections to Moliere's Work", *Physical Review*, Volume 115, p. 491, March 11, 1959.

10. Spencer, L.V., "Theory of Electron Penetration", *Physical Review*, Volume 98, p. 1597, January 20, 1955.

11. Fano, U. "Inelastic Collisions and the Moliere Theory of Multiple Scattering", *Physical Review*, Volume 93, p. 117, August 27, 1953.

12. Bethe, H.A., "Moliere's Theory of Multiple Scattering", *Physical Review*, Volume 89, p. 1256, November 28, 1952.

13. Keller, F.L., and Zerby, C.D., "Electron Transport Theory, Calculations, and Experiments", *Nuclear Science and Engineering*, Volume 27, p. 190, September 30, 1966.

14. Hanson, A.O., "Measurement of Multiple Scattering of 15.7-MeV Electrons", *Physical Review*, Volume 84, p. 634, July 3, 1951.

15. Kageyama, S., "The Multiple Scattering of Fast Electrons", *Journal of Phy. Soc. of Japan*, Volume 2, Number 4, p. 348, December 17, 1955.

16. Mozley, R.F., Smith, R.C., and Taylor, R.E., "Multiple Scattering of 600-MeV Electrons in Thin Foils", *Physical Review*, Volume 111, p. 647, March 31, 1958.

17. Halbleib, J.A., Kensek, R.P., *Version 2.1 of ITS*, ltr dated December 11, 1987.

INITIAL DISTRIBUTION LIST

11. Dr. Thomas A. Mehlhorn, Division 1265   1
    Sandia National Laboratories
    P.O. Box 5800
    Albuquerque, NM 87185

12. Dr. Kenneth J. Adams   1
    Science Applications International Corporation
    1710 Goodridge Drive, P.O. Box 1303
    McLean, VA 22102

13. Dr. Eugene Nolting   1
    White Oak Laboratory Stop H23
    Naval Surface Weapons Center
    10901 New Hampshire Ave
    Silver Spring, MD 20903-5000

14. Dr. Andy Smith   1
    White Oak Laboratory Stop H23
    Naval Surface Weapons Center
    10901 New Hampshire Ave
    Silver Spring, MD 20903-5000

15. Major C. Hill   1
    Defense Nuclear Agency
    Office RAEE
    Washington D.C. 20305-1000

16. LCDR L. Cohn   1
    Defense Nuclear Agency
    Office RAEE
    Washington D.C. 20305-1000

17. Theater Nuclear Warfare Program   1
    Naval Sea Systems Command
    PMS 423
    Washington D.C. 30362-5101

18. LCDR Robert J. Ross   1
    Defense Nuclear Agency
    Washington D.C. 20305

19. Dr. Norman J. Rudie   1
    IRT Corporation
    101 S. Kraemer Blvd., Suite 132
    Placentia, CA 92670

20. LT Daniel C Jensen   6
    2418 College S.E.
    Grand Rapids, MI 49507